THE JOURNAL OF PHYSICAL CHEMISTRY B

Article

pubs.acs.org/JPCB

General Strategy for Computing Nonlinear Optical Properties of Large Neutral and Cationic Organic Chromophores in Solution

Enrico Benassi,* Franco Egidi, and Vincenzo Barone*

Scuola Normale Superiore, Piazza dei Cavalieri 7, 56126 Pisa, Italy

Supporting Information

ABSTRACT: Tuning of nonlinear optical (NLO) properties of organic chromophores (OCs) by stereo-electronic and environmental effects has been widely documented by different experimental techniques and theoretical studies. Disentanglement and analysis of the different contributions requires, however, the availability of effective yet accurate quantum mechanical approaches for medium to large size systems in their natural environment. As a first step, we have shortly reviewed the phenomenological models still used by experimentalists to interpret their results and shown that a quantum mechanical approach based on the density functional theory (DFT) and the polarizable continuum model (PCM) should be able to overcome most theoretical limitations allowing, at the same time, the study of large systems with reasonable computational resources and the analysis of the results in terms of well-defined physical−chemical effects. After validation of the most suitable density functional/basis set in conjunction with the PCM description of bulk solvent effects, we have performed a systematic study of representative OCs, especially cationic ones, with special reference to their first order hyperpolarizability. The internal consistency of the results and their good agreement with experiment paves the route toward integrated experimental/computational studies of NLO properties taking together physical soundness, feasibility, reliability, and ease of interpretation.

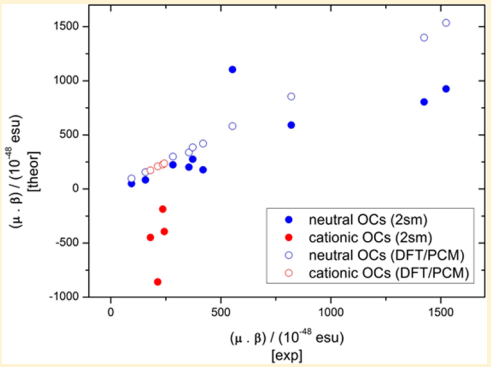

1. INTRODUCTION

In the last decade, materials showing nonlinear optical (NLO) properties have been the object of increasing attention by both experimental and computational points of view. NLO materials have important applications in different fields ranging from communications to medicine and are conventionally classified into inorganic and organic materials. Although inorganic systems (e.g., lithium niobate[1]) represent basic and widely employed materials for electro-optical devices for current optical communication systems, they have several disadvantages (for instance, high-quality single crystals are difficult to grow, are expensive, and are not easy to incorporate into electronic devices). As a consequence, attention has switched to organic chromophores (OC),[2,3] which show several advantages: (i) because of the purely electronic origin of their polarizability, response times are extremely fast (limited only by the electronic phase relaxation times of a few tens of femtoseconds); (ii) they are versatile so that the NLO properties can be custom-tailored to the particular needs of the specific application; (iii) they can be incorporated into a variety of macroscopic structures (Langmuir−Blodgett films, self-assembled films, and poled polymers, to produce solid-state NLO devices); (iv) they can be included within polymers, which are easy to be manufactured and integrated with semiconductor electronics;[4] (v) they have low dielectric constants and therefore reduced resistor−capacitor delay time constants and increased device bandwidths; and (vi) they have relatively constant refractive indices from the infrared to the microwave region and thus uniform behavior across that range. The investigation of a large number of organic π-conjugated molecules during the last 30 years has helped to establish general guidelines for the molecular design of good second-order NLO materials. However, a large number of extended π-conjugated organic molecules crystallize in centro-symmetric space groups, producing materials with no second-order bulk susceptibility. To overcome this problem, ionic and zwitterionic organic chromophores have emerged as important classes of materials for application in second-order NLO.[5−11]

As a matter of fact, a stilbazolium salt has shown the largest second harmonic generation (SHG) efficiency reported to date.[5] There are two main advantages in using ionic compounds for second-order NLO applications: (i) alignment of the ionic chromophore in a polar structure can be controlled by changing the counterion;[12−14] and (ii) dipolar interaction, which drives centro-symmetric arrangements that lack second-order bulk susceptibilities, is effectively countered by the Coulombic interaction, which favors non-centro-symmetric space groups that display good SHG efficiency. In particular, non-centro-symmetric stilbazolium co-crystals are very useful and highly efficient crystalline materials for electro-optic devices

Received: December 11, 2014
Revised: January 15, 2015

DOI: 10.1021/jp512342y
J. Phys. Chem. B XXXX, XXX, XXX−XXX

Chart 1. Neutral Organic Chromophores Containing Electron Donating ($-NH_2$, $-N(CH_3)_2$) and Electron Withdrawing ($-NO$, $-NO_2$, $-CN$, $-CHO$) Groups[a]

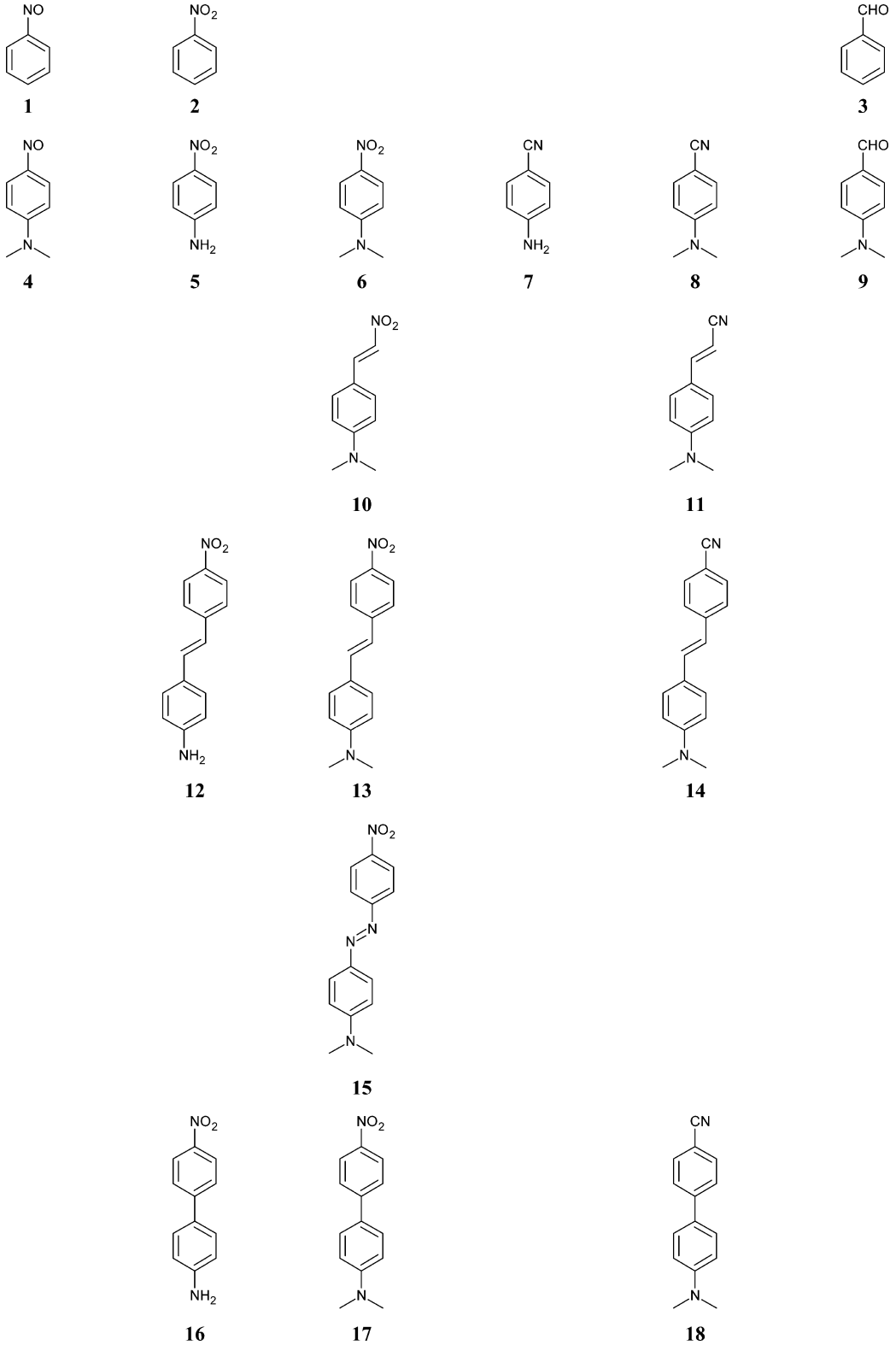

[a] **1**, nitrosobenzene; **2**, nitrobenzene; **3**, benzaldehyde; **4**, *p*-*N*,*N*-dimethylamino-nitrosobenzene; **5**, *p*-nitro-aniline; **6**, *p*-*N*,*N*-dimethylamino-nitrobenzene; **7**, *p*-amino-benzonitrile; **8**, *p*-*N*,*N*-dimethylamino-benzonitrile; **9**, *p*-*N*,*N*-dimethylamino-benzaldehyde; **10**, 4-*N*,*N*-dimethylamino-*β*-nitrostyrene; **11**, 4-*N*,*N*-dimethylamino-*β*-cyanostyrene; **12**, 4-amino-4′-nitrostilbene; **13**, 4-*N*,*N*-dimethylamino-4′-nitrostilbene; **14**, 4-*N*,*N*-dimethylamino-4′-cyanostilbene; **15**, 4-*N*,*N*-dimethylamino-4′-nitroazobenzene; **16**, 4-amino-4′-nitrobiphenyl; **17**, 4-*N*,*N*-dimethylamino-4′-nitrobiphenyl; **18**, 4-*N*,*N*-dimethylamino-4′-cyanobiphenyl.

DOI: 10.1021/jp512342y
J. Phys. Chem. B XXXX, XXX, XXX−XXX

because of their very high electro-optical coefficients coupled to a nearly perfect chromophoric orientation.[15,16] In addition, these co-crystals show remarkable physical properties (e.g., high melting point) together with linear and NLO properties which can be varied or tuned without modifying the chromophoric orientation in the crystal lattice, by changing the crystal growth conditions.

It is now well established that solvent polarity has a significant influence on the second-order NLO coefficients,[17−19] and this dependence on the local molecular environment is of immediate consequence for the rational design of chromophores and of solid-state devices incorporating these chromophores. Since the first-order hyperpolarizability (sometimes referred to as second-order polarizability) β of a chromophore is typically measured in just a single solvent, an accurate yet feasible computational modeling of solvent shifts on NLOs could be of paramount interest toward more efficient rational design strategies of purposely tailored compounds. Likewise, accurate modeling of the NLO properties of chromophores bound within macroscopic structures, such as those found in solid-state devices, would allow high through-put virtual screenings at reasonable costs.

During the past decade, we have assisted to an increasing development of computational techniques, in particular in the field of theoretical spectroscopy. Thanks to on-going developments of hardware and software, the accuracy of computed NLO molecular properties rivals that of their experimental counterparts for small semi-rigid molecules in the gas phase.[20−24] It could, therefore, appear that quantum mechanical (QM) computations of second-order NLO properties of molecular chromophores can be considered a mature field. The situation is, however, more involved whenever molecular flexibility and environmental (e.g., solvent) effects come into play, as is the case for most situations of current technological or biological interest.[25] Under such circumstances, phenomenological models and/or strongly approximated computational approaches are still actively used to interpret experimental results.[26] On these grounds, a first aim of the present study is to analyze the approximations of the most used phenomenological models in the light of more rigorous treatments. Next, a computational strategy based on methods and models implemented in widely used QM packages is sought, which could be used also by non-specialists to parallel experimental studies of NLO properties for large systems in condensed phases without requiring prohibitive computer resources. Of course, a number of effects (e.g., vibrational averaging, full convergence with the basis set, and full account of correlation, dynamical solvent effects)[23,27,28] are lost in this simplification, but it is hoped that general trends and even semi-quantitative agreement with experiment can be still reached. In this connection, methods rooted in the density functional theory (DFT) and its time-dependent (TD-DFT) extension appear particularly effective provided that the specific functional and basis set are carefully selected[29,30] and coupled to last generation continuum solvent models (e.g., the polarizable continuum model (PCM)[31−33]) to take bulk solvent effects in the proper account for both structural and electric properties. In the following, this computational strategy is validated for some reference systems (Chart 1), leading to the selection of the most effective parameters (density functional, basis set, solvent cavity shape and dimension, description of local fields, etc.). To this end, we have selected 18 systems (Chart 1), which have been extensively investigated from an experimental point of view. They can be classified as push−pull molecules, with a general structure D−π−A, where D is an electron-donating group (amino or dimethyl-amino; in the cases **1** to **3**, the phenyl ring itself acts as donor) and A is an electron-withdrawing group (nitroso, nitro, nitrile, and aldehyde); D and A are connected through an aromatic/conjugated moiety of different sizes (phenyl, styril, stilbene, azobenzene, biphenyl). The best model issuing from this analysis is next applied to the description of NLO properties for a panel of neutral and cationic organic chromophores (NOC and COC, respectively; Chart 2), paying particular attention to the role of stereo-electronic and solvent effects in tuning the first hyperpolarizability.

Chart 2. Neutral and Cationic Organic Chromophores

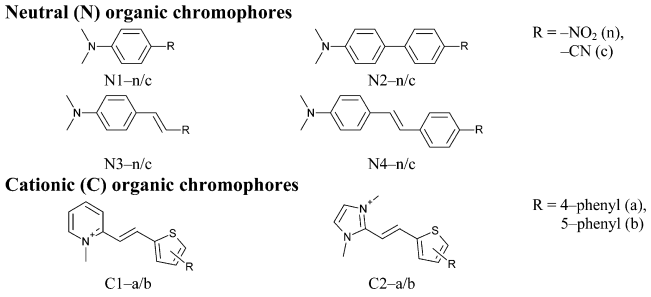

The paper is organized as follows. After this Introduction (Section 1), Section 2 contains a short review of the physical and theoretical background of NLOs, whereas the next two sections are devoted to short overviews of the main problems facing a reliable evaluation of solvatochromic effects on first hyperpolarizabilities (Section 3) and of the ability of last generation continuum solvent models to overcome the main difficulties of more traditional approaches based on the Onsager model including the proper treatment of solute shape and electronic density, together with non-equilibrium and local field effects (Section 4). In the next part of the work, after sketching the main building blocks of our computational strategy (Section 5), we present and analyze the results (Section 6), starting from the selection of the most suitable computational model and then proceeding to its validation and application to a quite large panel of systems and solvents. Finally, Section 7 summarizes conclusions and further perspectives.

2. GENERAL PHYSICAL BACKGROUND

The energy of a molecular system immersed in an electric field **E** can be expanded in a Taylor series about the field strength,

$$\varepsilon = \varepsilon_0 - \boldsymbol{\mu}\cdot\mathbf{E} - \frac{1}{2}\boldsymbol{\alpha}:\mathbf{E}^2 - \frac{1}{3!}\boldsymbol{\beta}\therefore\mathbf{E}^3 - \ldots \quad (1)$$

where we introduce the permanent electric dipole moment $\boldsymbol{\mu}$, the polarizability $\boldsymbol{\alpha}$, and the (first) hyperpolarizability $\boldsymbol{\beta}$:

$$\mu_i \equiv -\left(\frac{\partial\varepsilon}{\partial E_i}\right)_0 \quad (2a)$$

$$\alpha_{ij} \equiv -\left(\frac{\partial^2\varepsilon}{\partial E_i\partial E_j}\right)_0 = \left(\frac{\partial\mu_i}{\partial E_j}\right)_0 \quad (2b)$$

and

$$\beta_{ijk} \equiv -\left(\frac{\partial^3\varepsilon}{\partial E_i\partial E_j\partial E_k}\right)_0 = \left(\frac{\partial^2\mu_i}{\partial E_j\partial E_k}\right)_0 = \left(\frac{\partial\alpha_{ij}}{\partial E_k}\right)_0 \quad (2c)$$

DOI: 10.1021/jp512342y
J. Phys. Chem. B XXXX, XXX, XXX−XXX

The same quantities arise if we expand in Taylor's series the electric dipole moment $\boldsymbol{\mu}$ with respect to the electric field $\mathbf{E}$,

$$\boldsymbol{\mu} = \boldsymbol{\mu}_0 + \boldsymbol{\alpha}\cdot\mathbf{E} + \frac{1}{2}\boldsymbol{\beta}:\mathbf{E}^2 + \dots \tag{3}$$

We underline that consistently with Taylor's expansions 1 and 3 the polarizability and hyperpolarizability do not include the 1/2 and 1/3! factors used by some authors.[34] The first hyperpolarizability $\boldsymbol{\beta}$ is a third rank tensor that can be described by a $3 \times 3 \times 3$ matrix, whose 27 components can be reduced to 10 assuming Kleinman's symmetry,[35] i.e., $\beta_{ijj} = \beta_{jij} = \beta_{jji}$. The hyperpolarizability is often reported in the scalar form $\beta_{\parallel}$ (the component parallel to the electric field direction) or in vector form along the direction of the dipole moment $\boldsymbol{\beta}_{\mathrm{vec}}$.[36] Using the $\boldsymbol{\beta}$ tensor Cartesian components, the $\boldsymbol{\beta}_{\mathrm{vec}}$ Cartesian components can be calculated as follows,

$$\beta_i = \beta_{iii} + \frac{1}{3}\sum_{i\neq j}(\beta_{ijj} + \beta_{jij} + \beta_{jji}) \tag{4}$$

where $i, j = x, y, z$, whereas the vector magnitude can be defined as[37]

$$\begin{aligned}\beta &= [\beta_x^{\,2} + \beta_y^{\,2} + \beta_z^{\,2}]^{1/2} \\ &= [(\beta_{xxx} + \beta_{xyy} + \beta_{xzz})^2 + (\beta_{yxx} + \beta_{yyy} + \beta_{yzz})^2 \\ &\quad + (\beta_{zxx} + \beta_{zyy} + \beta_{zzz})^2]^{1/2}\end{aligned} \tag{5}$$

In a field which has a static and a dynamic (time dependent) component,

$$\mathbf{E} = \mathbf{E}^0 + \mathbf{E}^{\omega}e^{i\omega t} \tag{6}$$

the electric dipole moment is expanded as

$$\begin{aligned}\mu_i = \mu_{0i} &+ \sum_j \alpha_{ij}(0,0)E_j^0 + \sum_j \alpha_{ij}(-\omega,\omega)E_j^{\omega}e^{i\omega t} + \\ &+ \frac{1}{2}\sum_j\sum_k \beta_{ijk}(0;0,0)E_j^0E_k^0 + \frac{1}{4}\sum_j\sum_k \beta_{ijk}(0;\omega,-\omega)E_j^{\omega}E_k^{\omega} + \\ &+ \sum_j\sum_k \beta_{ijk}(-\omega;0,\omega)E_j^0E_k^{\omega}e^{i\omega t} \\ &+ \frac{1}{4}\sum_j\sum_k \beta_{ijk}(-2\omega;\omega,\omega)E_j^{\omega}E_k^{\omega}e^{2i\omega t} + \dots\end{aligned} \tag{7}$$

where $\boldsymbol{\alpha}(-\omega,\omega)$ is the frequency-dependent polarizability. There are three different frequency dependent first hyperpolarizabilities. Two of these are related, since

$$\beta_{ijk}(0;\omega,-\omega) = \beta_{kij}(-\omega;0,\omega) \tag{8}$$

The third quantity $\boldsymbol{\beta}(-2\omega;\omega,\omega)$ is responsible for frequency doubling. From a QM point of view, the polarizability can be written using a sum-over-state (SOS) formalism involving all exact eigenstates of the unperturbed system (i.e., in the absence of external fields).[38−40] However, the general SOS expression cannot be directly employed in QM calculations because, in principle, an infinite number of states should be included. In practice, in the case of charge-transfer systems like the ones considered in this work, the sum is often truncated to only include the ground and charge-transfer (CT) states. If we apply the two-state model, we have

$$\beta_{2\mathrm{sm}}(-\omega_1-\omega_2;\omega_1,\omega_2) = \beta_0 D(\omega_1,\omega_2) \tag{9}$$

where

$$\beta_0 = 3\frac{\mu_{\mathrm{eg}}^{\,2}(\mu_{\mathrm{e}} - \mu_{\mathrm{g}})}{W_{\mathrm{eg}}^{\,2}} \tag{10}$$

and

$$D(\omega_1,\omega_2) = \frac{1 - \frac{\omega_1\omega_2}{\omega_{\mathrm{eg}}^{\,2}}}{\left[1 - \left(\frac{\omega_1}{\omega_{\mathrm{eg}}}\right)^2\right]\left[1 - \left(\frac{\omega_2}{\omega_{\mathrm{eg}}}\right)^2\right]\left[1 - \left(\frac{\omega_1+\omega_2}{\omega_{\mathrm{eg}}}\right)^2\right]} \tag{11}$$

where $\beta_{2\mathrm{sm}}$ is the first hyperpolarizability issuing from the two-state perturbative model; β_0 represents here the static hyperpolarizability, μ_{g} and μ_{e} the *moduli* of the dipole moments of ground and excited (CT) states, μ_{eg} the *modulus* of the transition dipole moment between the two states, and $W_{\mathrm{eg}} = \hbar\omega_{\mathrm{eg}}$ the excitation energy of the excited (CT) state; D which represents the dispersion effect, is a function of frequencies of external field. For the Kerr effect, it reads:

$$D(\omega,0) = \frac{1}{\left[1 - \left(\frac{\omega}{\omega_{\mathrm{eg}}}\right)^2\right]^2} \tag{12}$$

whereas, for the SHG case, it becomes

$$D(\omega,\omega) = \frac{1}{\left[1 - \left(\frac{\omega}{\omega_{\mathrm{eg}}}\right)^2\right]\left[1 - \left(2\frac{\omega}{\omega_{\mathrm{eg}}}\right)^2\right]} \tag{13}$$

This is strictly related to the well-known Oudar's relation, which in its original form[41,42] looks like

$$\beta_{\mathrm{ct}} = 3\frac{e^2\hbar^2}{2m}\frac{W}{[W^2 - (\hbar\omega)^2][W^2 - (2\hbar\omega)^2]}f\Delta\mu_{\mathrm{ex}} \tag{14}$$

where

$$\begin{aligned}&W = \hbar\omega_{01} \\ &\Delta\mu_{\mathrm{ex}} = e(\langle 1|\mathbf{r}|1\rangle - \langle 0|\mathbf{r}|0\rangle) \\ &f = \frac{2m}{\hbar^2}W|\langle 0|\mathbf{r}|1\rangle|^2 = \frac{2m}{\hbar^2}Wr_{01}^{\,2} = \frac{2m}{\hbar^2}W\frac{\mu_{01}^{\,2}}{e^2} \\ &\quad = \frac{2m}{e^2\hbar^2}W\mu_{01}^{\,2}\end{aligned} \tag{15}$$

with $|0\rangle \equiv |g\rangle$ and $|1\rangle \equiv |e\rangle$. This expression is not strictly equal to the previous one (eq 9) possibly due to a mistyping. We have reported the definition of $\Delta\mu_{\mathrm{ex}}$ as it appears in the original paper; however, $\Delta\mu_{\mathrm{ex}}$ is a scalar quantity, whereas on the right side of the expression we have the difference of two vector quantities. With the notation $\langle a|\mathbf{r}|b\rangle$ the author indicates—as conventionally assumed—a vector; we understand this because he specifies $|\langle 0|\mathbf{r}|1\rangle|^2$ in the definition of the oscillator strength f. The expression of $\Delta\mu_{\mathrm{ex}}$ is thus ambiguous, since we could simply ask ourselves whether we have to use

$$\Delta\mu_{\mathrm{ex}} = e|\langle 1|\mathbf{r}|1\rangle - \langle 0|\mathbf{r}|0\rangle| = e|\mathbf{r}_1 - \mathbf{r}_0| = |\boldsymbol{\mu}_1 - \boldsymbol{\mu}_0| \tag{16}$$

or

$$\Delta\mu_{\mathrm{ex}} = e(|\langle 1|\mathbf{r}|1\rangle| - |\langle 0|\mathbf{r}|0\rangle|) = e(r_1 - r_0) = \mu_1 - \mu_0 \tag{17}$$

Since the static hyperpolarizability can also be negative (e.g., the chloroform has $\beta_0 = -(0.49 \pm 0.05) \times 10^{-30}$ esu),[43,44] we

DOI: 10.1021/jp512342y
J. Phys. Chem. B XXXX, XXX, XXX−XXX

conclude that the correct interpretation is $\Delta\mu_{ex} = \mu_1 - \mu_0$. Additionally, it is easy to prove that if $\Delta\mu_{ex} = \mu_1 - \mu_0$, then Oudar's equation coincides with the general expression of β_{2sm}, for the SHG case. After simple substitutions, we can also obtain the formula

$$\beta_{ct} = \frac{3\mu_{01}^{2}\Delta\mu_{ex}}{\hbar^2}\frac{\omega_{01}^{2}}{[\omega_{01}^{2} - \omega^2][\omega_{01}^{2} - 4\omega^2]} \qquad (14')$$

where $\Delta\mu_{ex} \equiv \mu_1 - \mu_0$ is the difference of *moduli* of the electric dipole moments of the excited stated $|1\rangle$ and of the ground state $|0\rangle$. In the literature one can find slightly different expressions,[45−51] depending on the chosen units and whether to include the Taylor expansion factors within the hyperpolarizability. Moreover, the details of Oudar's equation are often omitted, the static case ($\hbar\omega = 0$ eV) is assumed, and the following two-state expression is found:

$$\beta \propto \frac{r_{ge}^{2}(\mu_{ee} - \mu_{gg})}{E_{ge}^{2}} \qquad (14'')$$

The two-state expressions imply that frequency doubling will be enhanced near resonance either of the single photon or the two-photon type or by increasing the oscillator strength or charge-transfer character of the important transition.

In this work, we will refer only to Oudar's equation. If other states are either far from the CT state or have small oscillator strengths, their contributions to the dispersion are expected to be negligible. Furthermore, if the two-state model provides a reasonable description of the $\beta_{2sm}(-2\omega,\omega,\omega)$ dispersion, it can be safely assumed that for small ω

$$\beta_{est} = \beta_{2sm}(-2\omega, \omega, \omega) + \beta_{o.s.}(0, 0, 0) \qquad (18)$$

where $\beta_{o.s.}(0,0,0)$ represents the contributions from other states. The calculations can provide accurate results for the dipole moments of the ground and CT states. The critical quantity in the two-state model calculations is the excitation energy.

Although the two-state model has been largely employed in literature in view of its intuitive features and ease of use, it represents a strong simplification to the complete electrodynamical treatment of the NLO response and can thus lead to misleading conclusions, even when applied with critical sense.[52,53] Additionally, as pointed out by Zyss and Ledoux,[54] the two-state model is obviously not valid in the case of octopolar molecules, as it would lead to a strictly vanishing β as a result of the symmetry cancellation of ground and excited state dipolar moments. A three-state model has been proposed to overcome these difficulties, which leads to an expression for β strikingly similar to that of a two-state system and involves the ground state and a doubly degenerate excited state for the special case of trigonal systems.

Since, to the best of our knowledge, a detailed and systematic study about the reliability and applicability of the two-state model has not yet been performed for medium- to large-size systems, a first aim of the present study is to fill this gap. Furthermore, in the two-state model the solvent dependence of the hyperpolarizability is due to the solvent induced changes in the excitation energy to the CT state, the transition moment, and the dipole moment difference. Also these aspects will be analyzed in the following Sections.

3. SOLVATOCHROMIC SHIFTS

3.1. Experimental Determination of the First Hyperpolarizability. In the development of new materials, it is sometimes more convenient and appropriate to characterize the individual molecules composing the material rather than the bulk material itself. This is especially true for organic materials, since the bulk optical properties of organic crystals are largely determined by those of their individual molecular units. The most common methods for the characterization of molecular parameters include Electric Field Induced Second Harmonic Generation (EFISH or SHG), Hyper−Rayleigh Scattering (HRS), and Solvatochromatic Measurement (SCM) method.[55] The SCM is particularly effective for screening new NLO organic materials without performing any laser measurement. It is based on the two-state microscopic model of the first hyperpolarizability developed by Oudar and already mentioned in the previous section. The result of this model is an expression for β in terms of other measurable microscopic quantities (see eq 14). The transition wavenumber can be determined through an absorption spectrum measurement of the molecule. The transition dipole moment can be related to the area of the band under the spectrum:

$$\mu_{eg}^{2} = \frac{3e^2h}{8\pi^2mc}\frac{f}{\tilde{\nu}_{eg}} = \frac{3\ln 10\hbar c\varepsilon_0}{\pi N_A n}\frac{1}{\tilde{\nu}_{eg}}\int_{band}\varepsilon(\tilde{\nu})\,d\tilde{\nu} \qquad (19)$$

The most critical point consists in the (correct interpretation and) determination of $\Delta\mu_{ex} \equiv \mu_1 - \mu_0$. As clarified above, the quantity $\Delta\mu_{ex}$ is the difference between the *modulus* of the excited state electric dipole moment and the *modulus* of the ground state electric dipole moment. It is generally assumed that this quantity can be simply determined through solvatochromic measurements (in absorption or both absorption−emission spectra), but this hypothesis involves a number of difficulties. As a first point, the ground state dipole moment *modulus* must be obtained by other measurements, and in particular from concentration-dependent measurements of the static dielectric constant and the index of refraction with extrapolation to infinite dilution[56−62] (Guggenheim's method[57] was developed for apolar solvents) or electrochromic measurements. This is found in most of the (few) papers dealing with the SCM. The excited state dipole moment *modulus* can be obtained from electrochromic (absorption/emission) measurements. All of these techniques are fairly challenging and delicate and have strong limitations concerning the solvent and the molecular features of the system. Additionally, there exist techniques for the experimental (solvatochromic) measurement of the electric dipole moment of the excited state,[63−67] but there are two aspects that need to be stressed. Stokes' shift is interpreted on the basis of Lippert−Mataga,[68−70] McRae,[71] analogous first-principle,[72−74] or phenomenological[75] equations, which cannot be applied in general for any system, and when applicable provide values which are strongly affected by the assumptions and simplifications of the models (e.g., spherical cavity, solvent-independent dipole moments, etc.). Moreover, even if applicable, the above-mentioned solvatochromic relationships provide[76] $(\boldsymbol{\mu}_1 - \boldsymbol{\mu}_0)^2 = \mu_1^2 + \mu_0^2 - 2\mu_1\mu_0\cos\theta$. This means that, even when μ_0 has been determined through other measurements, it is not possible to obtain $\boldsymbol{\mu}_1$ without knowing the angle θ formed between the two vectors $\boldsymbol{\mu}_1$ and $\boldsymbol{\mu}_0$. Some other relationships have been proposed that involve the *moduli* of $\boldsymbol{\mu}_1$ and $\boldsymbol{\mu}_0$ and thus could be used for obtaining μ_1, once μ_0 is known (e.g., in the equation of

DOI: 10.1021/jp512342y
J. Phys. Chem. B XXXX, XXX, XXX−XXX

Kawski−Chamma−Vialler),[77,78] but actually they still make strong approximations for the description of the system and are not so widely employed for the interpretation of solvatochromism. Lippert−Mataga or McRae equations could be still used to obtain $\mu_1 - \mu_0$ whenever the two vectors $\boldsymbol{\mu}_1$ and $\boldsymbol{\mu}_0$ are collinear, but in order to verify this, QM calculations are still needed, and thus the solvatochromic measurements would lose utility, since the theoretical calculations would provide all the requested quantities.

Finally, we note that one of the largest sources of error in the SCM is the use of an effective (solvent-independent) radius for the cavity definition of the solute molecule in the solvent, because it enters as a cubed value in the solvatochromic *formulas*. For long conjugated molecules, for instance, the assumption of an equivalent sphere is inadequate. The SCM may work better for small, nearly spherical molecules (assumption that should be carefully evaluated). Although its accuracy is generally not as good as EFISH or HRS, in some simple cases SCM can be useful for qualitative screening of new organic materials of comparable size.

3.2. Modern Solvatochromic Models and Local Field Effects. As mentioned in the previous section, the interpretation of experimental solvatochromic shifts is often based on the simple Onsager model,[79] which reduces the solute molecule to a point dipole placed at the center of a spherical cavity carved within a dielectric continuum with given dielectric properties, which represents the solvent. This model rests on very strong approximations and, therefore, cannot yield quantitative results.[27,80−82] However, these limitations can be fully overcome by using more recent approaches, such as those rooted in the polarizable continuum model (PCM),[31,32] which treat the solute using its true charge density computed quantum-chemically (rather than reducing it to the sole dipole term) in the specific solvent, and employ a molecule-shaped cavity, rather than a spherical one. PCM can be effectively employed in the calculation of excited-state properties,[83] allowing the computation of the ground and excited state dipole moments, as well as the transition dipole moments, and can also be used directly in the computation of frequency-dependent polarizabilities of solvated systems.[33,84] PCM can also replace the Onsager−Lorentz model for the treatment of the local field effect, which accounts for the fact that the presence of the solvent not only affects the solute's properties directly but also affects the external electromagnetic field used to probe them, causing the local field acting on the solute to be different than the external field applied on the sample. It can be shown[79,80] that the external field acts on an effective dipole moment ($\boldsymbol{\mu}^*$), sum of the molecule dipole moment ($\boldsymbol{\mu}^{(m)}$), and the dipole moment arising from the molecule-induced dielectric polarization ($\boldsymbol{\mu}^{\S}$):

$$\boldsymbol{\mu}^*_{(s)} \equiv \frac{\partial G_{(s)}}{\partial \mathbf{E}^{(ext)}} = \boldsymbol{\mu}^{(m)}_{(s)} + \boldsymbol{\mu}^{\S}_{(s)} = f\boldsymbol{\mu}^{(m)}_{(s)} \tag{20}$$

where f is the local field factor, computed by taking the ratio of μ^* and $\mu^{(m)}$. Within the approximate Onsager−Lorentz electrostatic model (LO), which considers the molecule as a polarizable point dipole inside a spherical cavity, the local field factor is estimated as

$$f_{(LO)} = \frac{3\xi}{2\xi + 1} \quad \begin{cases} \xi = \varepsilon & \text{for static properties} \\ \xi = n^2 & \text{for dynamic properties} \end{cases} \tag{21}$$

This formulation is very simplified, resulting in a local field factor that only depends on the dielectric properties of the solvent, and is the same for every solute. In PCM, the effective dipole moment should replace the molecular dipole moment in the response calculations that yield the molecular (hyper)-polarizabilities;[27,81,82,85,86] however, the implementation in the case of hyperpolarizabilities, to the best of our knowledge, is not commonly available in any commercial Quantum Chemical code for general cavities. A simpler way to account for these effects is to compute the local field factor from eq 20 directly and use it to correct the other molecular properties.

Finally, in the case of dynamic molecular properties such as frequency-dependent hyperpolarizabilities, the dynamical aspects of solvation should also be considered. The laser frequencies employed in the experimental determinations usually lie in the visible−NIR region of the spectrum, with a period of oscillation in the order of femtoseconds. The solvent cannot follow the fast evolution of the solute charge density induced by the radiation with all its degrees of freedom; therefore, some of them remain static, entering a non-equilibrium configuration. This effect can be also included in PCM calculations, by separating the solvent polarization in two contributions, an equilibrium one (accounting for the "fast" degrees of freedom) and a non-equilibrium one (accounting for the degrees of freedom that can be considered slow with respect to the characteristic time scale of the perturbing electromagnetic field).[33,87,88] Within the nonequilibrium solvation regime, only fast solvent degrees of freedom are in equilibrium with the excited state electron density; within the equilibrium solvation regime, at infinite time, the solvent is fully equilibrated with the solute density. Note that within the PCM the fast and slow components are computed using the optical and static dielectric constants of the solvent, respectively.

4. QUANTUM CHEMICAL BACKGROUND

By using response theory, the first-order hyperpolarizability $\boldsymbol{\beta}(-2\omega;\omega,\omega)$ can be calculated without referring to the SOS method as[88]

$$\boldsymbol{\beta}(-2\omega;\ \omega,\ \omega) = -2\mathrm{Tr}[\boldsymbol{\mu}\cdot\mathbf{P}^{(2)}] \tag{22}$$

where $\boldsymbol{\mu}$ is the electric dipole moment integral matrix and $\mathbf{P}^{(2)}$ is the second-order density matrix. To obtain a generic second-order density matrix it is necessary to solve the perturbation equations up to second order; however, when only one dynamic perturbation is involved, as in the case of second harmonic generation, it is possible to avoid the resolution of the second-order equations by using an iterative procedure to reconstruct the density matrix.[89,90] The second-order density matrix results from the differentiation with respect to the local field acting on the solute system; therefore, in principle it should be computed with the inclusion of local field effects. If, however, local field effects are not directly included in the response calculations, the numerical value of $\boldsymbol{\beta}(-2\omega;\omega,\omega)$ can be corrected *a posteriori* as

$$\tilde{\boldsymbol{\beta}}(-2\omega;\ \omega,\ \omega) = f_{(PCM)}{}^2\boldsymbol{\beta}(-2\omega;\ \omega,\ \omega) \tag{23}$$

where f_{PCM} is computed from eq 20. The corrected value $|\tilde{\boldsymbol{\beta}}_{vec}|$ can then be directly compared to the experiments. Otherwise, the comparison between experimental and computed results can be done by evaluating the two scalar quantities $\boldsymbol{\mu}\beta_{\parallel}$ (from the experiments) and $\boldsymbol{\mu}^*\cdot\tilde{\boldsymbol{\beta}}_{vec}$ (from the calculations), respectively. In this study we have followed the former

DOI: 10.1021/jp512342y
J. Phys. Chem. B XXXX, XXX, XXX−XXX

Table 1. Comparison between the Computational Results for *p*-Nitroaniline, in Vacuo and in Solution (1,4-dioxane), at DFT/PCM(UFF) Level, Employing the aug-cc-pVTZ Basis Set and Different Functionals

		μ, D					α_{iso}, 10^{-24} cm^3								$\beta_{\parallel}$, 10^{-30} esu							
		vacuum		1,4-dioxane			vacuum		1,4-dioxane						vacuum		1,4-dioxane					
									a		*b*		*c*				*a*		*b*		*c*	
functional	ω, eV	*a*	*b*	*a*	*b*	*c*	*a*	*b*	*d*	*e*	*d*	*e*	*d*	*e*	*a*	*b*	*d*	*e*	*d*	*e*	*d*	*e*
B3LYP	0.0000	5.69	5.76	7.09	6.95	7.19	15.94	15.97	18.91	20.94	18.85	20.88	18.96	21.00	28.67	29.08	27.62	33.88	28.06	34.42	27.92	34.25
	0.6502						16.06	16.09	18.83	20.68	18.77	20.62	18.88	20.73	33.91	34.39	31.90	38.50	32.45	39.15	32.24	38.91
	0.6561						16.06	16.09	18.83	20.68	18.77	20.62	18.88	20.74	34.01	34.52	32.01	38.64	32.58	39.28	32.38	39.05
	0.9051						16.18	16.21	19.01	20.88	18.95	20.82	19.07	20.94	40.47	41.09	39.05	47.11	39.79	47.99	39.52	47.68
	1.1698						16.35	16.38	19.28	21.18	19.22	21.11	19.34	21.24	53.47	54.35	54.28	65.51	55.47	66.94	55.07	66.43
	1.3626						16.51	16.54	19.54	21.46	19.48	21.39	19.60	21.53	71.80	73.16	78.43	94.62	80.51	97.10	79.86	96.32
	1.4940						16.64	16.68	19.75	21.69	19.68	21.62	19.82	21.77	94.42	96.49	113.26	136.66	116.93	141.08	115.95	139.86
PBE0	0.0000	5.55	5.71	6.88	6.87	7.10	15.56	15.75	18.37	20.36	18.55	20.55	18.66	20.67	25.78	27.55	24.83	30.51	26.53	32.55	26.53	32.55
	0.6502						15.66	15.86	18.27	20.08	18.46	20.28	18.57	20.40	30.00	32.24	28.20	34.08	30.30	36.56	30.30	36.56
	0.6561						15.67	15.87	18.28	20.09	18.46	20.28	18.57	20.40	30.10	32.35	28.30	34.18	30.41	36.70	30.41	36.70
	0.9051						15.77	15.97	18.43	20.26	18.63	20.46	18.74	20.59	35.20	38.06	33.81	40.85	36.60	44.18	36.60	44.18
	1.1698						15.92	16.13	18.66	20.51	18.87	20.73	18.99	20.86	45.07	49.22	45.13	54.52	49.52	59.79	49.56	59.79
	1.3626						16.06	16.28	18.88	20.75	19.10	20.98	19.23	21.12	58.13	64.32	61.53	74.32	68.81	83.02	68.91	83.16
	1.4940						16.17	16.40	19.06	20.95	19.29	21.19	19.42	21.33	72.96	81.90	82.34	99.45	94.25	113.74	94.59	114.14
CAM-B3LYP	0.0000	5.39	5.57	6.61	6.65	6.89	15.29	15.50	17.96	19.91	18.18	20.14	18.31	20.28	24.32	26.26	23.81	29.25	25.30	31.05	25.95	31.84
	0.6502						15.38	15.60	17.86	19.63	18.08	19.86	18.21	20.00	27.82	30.20	26.63	32.18	28.43	34.35	29.18	35.20
	0.6561						15.38	15.61	17.86	19.63	18.08	19.86	18.21	20.01	27.92	30.30	26.70	32.24	28.54	34.45	29.28	35.34
	0.9051						15.47	15.70	18.00	19.78	18.22	20.02	18.36	20.17	31.97	34.90	31.22	37.72	33.57	40.51	34.49	41.63
	1.1698						15.60	15.84	18.20	20.00	18.43	20.25	18.58	20.41	39.49	43.54	40.00	48.33	43.47	52.48	44.86	54.11
	1.3626						15.73	15.97	18.39	20.21	18.63	20.47	18.79	20.64	48.77	54.42	51.70	62.45	56.94	68.74	59.08	71.29
	1.4940						15.82	16.08	18.54	20.37	18.79	20.65	18.95	20.82	58.57	66.12	65.10	78.60	72.82	87.89	75.98	91.70
M06-2X	0.0000	5.32	5.58	6.51	6.65	6.88	15.09	15.34	17.68	19.60	17.95	19.89	18.08	20.03	21.67	24.32	21.36	26.26	23.54	28.91	24.22	29.73
	0.6502						15.17	15.43	17.57	19.32	17.85	19.61	17.98	19.75	24.83	27.99	23.81	28.74	26.36	31.80	27.14	32.75
	0.6561						15.18	15.43	17.57	19.32	17.85	19.61	17.98	19.76	24.90	28.09	23.88	28.84	26.43	31.90	27.24	32.86
	0.9051						15.26	15.53	17.70	19.46	17.99	19.76	18.12	19.91	28.40	32.21	27.72	33.50	30.92	37.31	31.94	38.54
	1.1698						15.38	15.66	17.88	19.66	18.19	19.98	18.33	20.14	34.73	39.86	35.07	42.34	39.62	47.82	41.09	49.59
	1.3626						15.50	15.78	18.06	19.85	18.37	20.19	18.53	20.35	42.41	49.35	44.52	53.81	51.12	61.70	53.33	64.35
	1.4940						15.59	15.88	18.20	20.00	18.52	20.35	18.68	20.52	50.34	59.32	54.96	66.43	64.21	77.51	67.41	81.32
ωB97X	0.0000	5.14	5.39	6.27	6.41	6.64	15.06	15.29	17.60	19.52	17.86	19.80	17.99	19.94	20.92	23.54	20.44	25.13	22.55	27.69	23.47	28.81
	0.6502						15.14	15.38	17.49	19.23	17.75	19.51	17.89	19.65	23.37	26.50	22.35	27.01	24.79	29.96	25.85	31.22
	0.6561						15.15	15.38	17.49	19.23	17.75	19.51	17.89	19.66	23.40	26.53	22.41	27.07	24.86	30.03	25.92	31.32

J. Phys. Chem. B XXXX, XXX, XXX−XXX DOI: 10.1021/jp512342y

Table 1. continued

functional	ω, eV	μ, D					$\alpha_{iso\omega}$, 10^{-24} cm^3										$\beta_{\parallel}$, 10^{-30} esu									
		vacuum		1,4-dioxane			vacuum		1,4-dioxane								vacuum		1,4-dioxane							
		a	b	a	b	c	a	b	a	e	b	d	e	c	d	e	a	b	a	e	b	d	e	c	d	e
	0.9051						15.23	15.47	17.61	19.36	17.88	19.65	18.02	19.80			26.46	30.17	25.71	31.09	28.74	34.73	30.07	36.29		
	1.1698						15.34	15.60	17.78	19.55	18.06	19.85	18.21	20.01			31.87	36.73	31.87	38.54	36.05	43.54	37.89	45.75		
	1.3626						15.45	15.71	17.94	19.72	18.23	20.04	18.39	20.21			38.23	44.62	39.56	47.79	45.37	54.79	47.96	57.92		
	1.4940						15.53	15.80	18.07	19.86	18.37	20.19	18.54	20.37			44.62	52.68	47.68	57.62	55.54	67.07	59.11	71.36		

[a]Properties calculated after geometry optimization at the same level. [b]Properties calculated assuming the geometry optimized at B3LYP/6-31+G* level in vacuo. [c]Properties calculated assuming the geometry optimized at B3LYP/6-31+G* level in 1,4-dioxane. [d]Without local field correction. [e]With local field correction.

choice for the benchmarking, the latter one for the applications (vide infra).

5. COMPUTATIONAL DETAILS

As hinted in the Introduction, our investigation is based on DFT and PCM models in the frame of methods fully available in commercial quantum chemical packages (Gaussian,[91] in the present context). We have considered two sets of chromophores, dedicated to the benchmarking (Chart 1) and to the applications (Chart 2). All the systems have been previously investigated in experimental literature, and some of them also computationally.

In a first step, a panel of 18 neutral chromophores (Chart 1) was used to perform an extensive benchmark study using hybrid (B3LYP,[92] PBE0,[93] and M06-2X[94]) and long-range corrected (CAM-B3LYP[95] and ωB97X[96]) functionals, in conjunction with different basis sets. In particular, we have employed double- and triple-ζ Pople-, Dunning-, and Barone-type sets, viz., 6-31+G*, 6-311++G**, aug-cc-pVDZ, aug-cc-pVTZ,[97−103] SNSD, and SNST.[104] The calculations were run both in vacuo and in solvent. The IEF-PCM polarizable continuum model[105,106] has been used to describe bulk solvent effects testing different sets of effective *radii* (Universal Force Field (UFF),[107] Pauling−Merz−Singh−Kollman's (PMSK)[108] and Bondi's (B)[109]) for building the solvent cavity and static and optical dielectric constants according to Gaussian 09 defaults. The calculations consist in a two-step protocol: (1) to optimize the molecular geometry and to perform a vibrational frequency calculation to verify that the reached point is a "genuine" minimum of the potential energy hypersurface and (2) to calculate the properties, viz., the ground state electric dipole moment ($\boldsymbol{\mu}_0$) and the static and dynamic dipole polarizability ($\boldsymbol{\alpha}$) and first-order hyperpolarizabilities ($\boldsymbol{\beta}$) for the molecules in the electronic ground state, the $S_n \leftarrow S_0$ (n = 1−5) transition energies and the electric dipole moments for the excited states S_n ($\boldsymbol{\mu}_n$). For each single molecule, the dynamic properties were evaluated at the characteristic values of ω used in the EFISH experiments. In this step we have evaluated also the relevance of the geometry, both in vacuo and in solution, by performing a single point calculation of the properties at different levels of theory but keeping the same geometry as optimized using the 6-31+G* basis set.

Next, the most effective model (functional, basis set, cavity *radii*, local field factors) obtained from the benchmarking has been used for the neutral and charged chromophores represented in Chart 2. For these cases, the comparison with the experimental data has been done considering the product $\boldsymbol{\mu}^*\cdot\tilde{\boldsymbol{\beta}}_{vec}$. Additionally, we have tested the reliability of the IEF-PCM with *radii* from Truhlar and co-workers' SMD solvation model,[90] which has never been employed for the prediction of electronic properties. To this aim, we have evaluated $\boldsymbol{\mu}^*\cdot\tilde{\boldsymbol{\beta}}_{vec}$ after both having re-optimized the geometries at the DFT/IEF-PCM (SMD) level and employing the geometries as obtained at DFT/IEF-PCM (UFF) level and performing a single point calculation of the properties with SMD.

6. RESULTS AND DISCUSSION

In the next section (6.1), we will present the results of our extended benchmarking for *p*-nitroaniline in vacuo and in 1,4-dioxane, a prototypical push−pull system. Then, in Section 6.2, the conclusions reached in the case of *p*-nitroaniline will be extended to a set of 18 OCs in different environments, and the

DOI: 10.1021/jp512342y
J. Phys. Chem. B XXXX, XXX, XXX−XXX

Table 2. Comparison between the Computational Results for *p*-Nitroaniline, in Vacuo and in Solution (1,4-dioxane), at DFT CAM-B3LYP/PCM(UFF) Level, Employing Different Basis Sets

		μ, D					α_{iso}, 10^{-24} cm^3								$\beta_{\|}$, 10^{-30} esu							
		vacuum		1,4-dioxane			vacuum		1,4-dioxane						vacuum		1,4-dioxane					
									a		*b*		*c*				*a*		*b*		*c*	
basis set	ω, eV	*a*	*b*	*a*	*b*	*c*	*a*	*b*	*d*	*e*	*d*	*e*	*d*	*e*	*a*	*b*	*d*	*e*	*d*	*e*	*d*	*e*
6-31+G*	0.0000	5.65	5.65	6.87	6.84	7.07	14.49	14.49	17.00	18.84	17.16	19.02	17.30	19.17	27.11	27.11	26.16	32.14	27.18	33.37	27.79	34.15
	0.6502						14.59	14.59	16.92	18.60	17.09	18.78	17.22	18.93	30.95	30.95	29.18	35.27	30.47	36.80	31.19	37.69
	0.6561						14.59	14.59	16.92	18.61	17.09	18.79	17.23	18.93	31.02	31.02	29.28	35.37	30.54	36.90	31.29	37.79
	0.9051						14.68	14.68	17.06	18.76	17.23	18.94	17.37	19.09	35.41	35.41	34.15	41.26	35.81	43.26	36.73	44.35
	1.1698						14.81	14.81	17.26	18.98	17.44	19.17	17.59	19.33	43.54	43.54	43.64	52.72	46.12	55.75	47.51	57.38
	1.3626						14.93	14.93	17.45	19.19	17.64	19.39	17.80	19.56	53.57	53.57	56.32	68.06	60.17	72.68	62.28	75.20
	1.4940						15.03	15.03	17.61	19.36	17.80	19.56	17.96	19.74	64.15	64.15	70.91	85.68	76.66	92.61	79.79	96.36
6-311+ +G**	0.0000	5.52	5.63	6.70	6.82	7.05	14.44	14.59	16.92	18.76	17.30	19.17	17.43	19.32	25.30	26.46	24.52	30.13	26.73	32.82	27.38	33.60
	0.6502						14.53	14.68	16.84	18.51	17.22	18.92	17.36	19.07	28.84	30.27	27.31	33.03	30.03	36.26	30.78	37.14
	0.6561						14.54	14.68	16.84	18.52	17.22	18.93	17.36	19.07	28.91	30.34	27.41	33.13	30.10	36.36	30.85	37.28
	0.9051						14.62	14.77	16.97	18.66	17.37	19.08	17.51	19.24	32.99	34.73	31.90	38.57	35.37	42.72	36.32	43.88
	1.1698						14.75	14.91	17.17	18.87	17.58	19.32	17.73	19.48	40.47	42.85	40.61	49.11	45.78	55.27	47.17	56.97
	1.3626						14.87	15.03	17.35	19.07	17.78	19.53	17.94	19.71	49.69	52.92	52.14	63.02	59.96	72.41	62.14	75.00
	1.4940						14.96	15.13	17.50	19.23	17.94	19.71	18.10	19.89	59.32	63.60	65.23	78.84	76.73	92.68	80.00	96.56
aug-cc-pVDZ	0.0000	5.31	5.43	6.51	6.65	6.88	15.13	15.36	17.75	19.67	18.24	20.20	18.37	20.34	22.62	23.98	22.38	27.52	24.79	30.44	25.44	31.19
	0.6502						15.22	15.45	17.64	19.39	18.14	19.93	18.27	20.07	25.78	27.48	24.93	30.10	27.86	33.64	28.60	34.49
	0.6561						15.22	15.46	17.65	19.40	18.14	19.93	18.27	20.07	25.85	27.55	25.00	30.20	27.96	33.74	28.67	34.62
	0.9051						15.31	15.55	17.78	19.54	18.28	20.09	18.42	20.23	29.56	31.60	29.11	35.17	32.86	39.66	33.81	40.78
	1.1698						15.44	15.68	17.97	19.75	18.49	20.32	18.64	20.47	36.29	39.11	36.97	44.66	42.55	51.32	43.94	52.99
	1.3626						15.55	15.80	18.14	19.94	18.69	20.53	18.85	20.70	44.52	48.43	47.28	57.11	55.71	67.21	57.82	69.76
	1.4940						15.64	15.90	18.29	20.10	18.85	20.71	19.01	20.88	53.13	58.30	58.87	71.12	71.15	85.85	74.32	89.66
aug-cc-pVTZ	0.0000	5.39	5.57	6.61	6.65	6.89	15.29	15.50	17.96	19.91	18.18	20.14	18.31	20.28	24.32	26.26	23.81	29.25	25.30	31.05	25.95	31.84
	0.6502						15.38	15.60	17.86	19.63	18.08	19.86	18.21	20.00	27.82	30.20	26.63	32.18	28.43	34.35	29.18	35.20
	0.6561						15.38	15.61	17.86	19.63	18.08	19.86	18.21	20.01	27.92	30.30	26.70	32.24	28.54	34.45	29.28	35.34
	0.9051						15.47	15.70	18.00	19.78	18.22	20.02	18.36	20.17	31.97	34.90	31.22	37.72	33.57	40.51	34.49	41.63
	1.1698						15.60	15.84	18.20	20.00	18.43	20.25	18.58	20.41	39.49	43.54	40.00	48.33	43.47	52.48	44.86	54.11
	1.3626						15.73	15.97	18.39	20.21	18.63	20.47	18.79	20.64	48.77	54.42	51.70	62.45	56.94	68.74	59.08	71.29
	1.4940						15.82	16.08	18.54	20.37	18.79	20.65	18.95	20.82	58.57	66.12	65.10	78.60	72.82	87.89	75.98	91.70
SNSD	0.0000	5.38	5.58	6.59	6.67	6.91	15.27	15.56	17.93	19.86	18.25	20.21	18.38	20.36	24.05	26.33	23.67	29.08	25.51	31.29	26.16	32.07
	0.6502						15.36	15.67	17.83	19.59	18.15	19.94	18.29	20.08	27.52	30.30	26.46	31.94	28.67	34.59	29.42	35.47
	0.6561						15.36	15.67	17.83	19.59	18.16	19.94	18.29	20.09	27.58	30.37	26.53	32.04	28.77	34.73	29.49	35.58
	0.9051						15.45	15.77	17.97	19.74	18.30	20.10	18.44	20.25	31.56	35.00	30.98	37.41	33.84	40.85	34.79	41.97
	1.1698						15.58	15.91	18.16	19.96	18.51	20.34	18.66	20.50	38.91	43.71	39.62	47.85	43.91	52.99	45.30	54.62
	1.3626						15.70	16.04	18.35	20.17	18.72	20.56	18.87	20.73	48.02	54.69	51.12	61.73	57.65	69.59	59.79	72.11
	1.4940						15.80	16.15	18.50	20.33	18.88	20.74	19.04	20.91	57.58	66.56	64.25	77.58	73.91	89.18	77.10	92.99
SNST	0.0000	5.35	5.59	6.56	6.67	6.91	15.12	15.50	17.75	19.68	18.17	20.13	18.30	20.27	23.91	26.56	23.47	28.81	25.68	31.49	26.29	32.28

DOI: 10.1021/jp512342y

Table 2. continued

basis set	ω, eV	μ, D					α_{iso}, 10^{-24} cm^3						$\beta_{\parallel}$, 10^{-30} esu					
		vacuum		1,4-dioxane			vacuum		1,4-dioxane				vacuum		1,4-dioxane			
		a	b	a	b	c	a	b	a	b	c		a	b	a	b	c	
									d	e	d	e	d	e	d	e	d	e
	0.6502						15.22	15.60	17.65	19.40	18.08	19.86	18.21	20.00	27.31	30.54	26.19	31.63	28.84	34.83	29.59	35.71
	0.6561						15.22	15.60	17.66	19.40	18.08	19.86	18.21	20.00	27.38	30.64	26.26	31.70	28.94	34.93	29.69	35.81
	0.9051						15.31	15.70	17.79	19.55	18.22	20.02	18.36	20.17	31.29	35.30	30.61	36.97	34.05	41.09	35.00	42.21
	1.1698						15.43	15.84	17.98	19.76	18.44	20.25	18.58	20.41	38.47	44.05	39.05	47.14	44.15	53.30	45.58	54.96
	1.3626						15.55	15.97	18.16	19.96	18.64	20.47	18.79	20.64	47.34	55.13	50.17	60.58	57.99	69.96	60.13	72.58
	1.4940						15.65	16.08	18.31	20.12	18.80	20.65	18.96	20.83	56.63	67.14	62.79	75.85	74.35	89.72	77.58	93.60

[a]Properties calculated after geometry optimization at the same level. [b]Properties calculated assuming the geometry optimized at B3LYP/6-31+G* level in vacuo. [c]Properties calculated assuming the geometry optimized at B3LYP/6-31+G* level in 1,4-dioxane. [d]Without local field correction. [e]With local field correction.

results will be compared with available experimental data. Finally in Section 6.3, the reliability of the method will be tested for four additional cationic systems.

6.1. Selection and Validation of Models and Parameters. In this section, we will describe the results obtained for the *p*-nitroaniline (molecule **5** in Chart 1) in vacuo and in dioxane as a test case, in order to evaluate the effects of the functional, of the basis set, and of the solvent description. We have calculated the ground state electric dipole moment μ, the static and dynamic isotropic polarizability α_{iso}, and the static and dynamic SHG (first) hyperpolarizability $\beta_{\parallel}$, both in vacuo and in solution. The dynamic properties have been evaluated at ω = 0.6502 eV (λ = 1907 nm), 0.6561 eV (λ = 1890 nm), 0.9051 eV (λ = 1370 nm), 1.1698 eV (λ = 1064 nm), 1.3626 eV (λ = 910 nm), and 1.4940 eV (λ = 830 nm). These are the characteristic values of the EFISH experiments. The electric properties have been evaluated both after a full geometry optimization and assuming the B3LYP/6-31+G* geometry fixed (in vacuo and in solution). For the *p*-nitroaniline, as well as for all the systems of Chart 1 (see next paragraph), the importance of the local field effects are also evaluated. The complete collection of the results is available in the Supporting Information, Table SI.1. For the sake of shortness, here we show two extracts: Table 1, reporting the comparison between the computational results obtained employing different functionals, keeping fixed the basis set (aug-cc-pVTZ), whereas in Table 2 we compare the results obtained by the CAM-B3LYP functional only, employing different basis sets. The computational results are encouraging.

Concerning the choice of the functional (Table 1), if we look at the dipole moments, the obtained values are coherent and decrease when passing from B3LYP to PBE0, to CAM-B3LYP, to M06-2X, to ωB97X, both in vacuo and in solution (the experimental measurements of the electric dipole moment report values ranging between 6.1 and 7.1 D, see Table 3). In general the long-range corrected functionals give better results than the hybrid ones. The PBE0 and CAM-B3LYP functionals give balanced values, and it is confirmed that CAM-B3LYP is particularly suitable for this system.[110−112] It can also be noted that the difference between the values computed in solvent and in vacuo is not very sensitive to the functional employed. Analogous conclusions can be underlined for the static and dynamic isotropic polarizability. In the case of the hyperpolarizability, the differences are larger for the dynamic property, especially at high frequency.

Regarding the choice of the basis sets (Table 2), as is well-known, diffuse polarization functions are mandatory for obtaining converged electric properties, especially polarizabilities and hyperpolarizabilities. This is the reason why Pople-type bases do not work efficiently for predicting the properties: The 6-311++G** basis set, although improving 6-31+G* results, is still quite far from the aug-cc-pVTZ results. The best results are obtained with the SNST basis, even though this basis set may be inconvenient due to its quite large dimension. At the same time, in spite of its quite reduced cost, the aug-cc-pVDZ and SNSD sets lead to very good agreement with the aug-cc-pVTZ reference. Finally, it can be seen that the 6-31+G* basis set can be employed for the optimization of the geometry, especially when the system is of large size, and the further calculation of the properties can be done at a more appropriate level of theory. This is supported by the results in Figure 1, where we plot the static and dynamic values of $\beta_{\parallel}$ calculated recovering the geometry optimized at

DOI: 10.1021/jp512342y
J. Phys. Chem. B XXXX, XXX, XXX−XXX

Table 3. Collection of the Experimental Data for the Organic Chromophores of Chart 1 in Solution: Ground-to-Excited State Transition Wavenumber (ν_{eg} in kK = 10^3 cm^{-1}), Ground State Electric Dipole Moment (μ_g in D = 10^{-18} esu), Excited State Electric Dipole Moment (μ_e in D), Ground-to-Excited State Transition Electric Dipole Moment (μ_{eg} in D), Laser Wavelength (λ_L in nm), and First Hyperpolarizability (in 10^{-30} esu) As Obtained from Direct Measurements (β)

	solvent		μ_g, D		μ_e, D					$\mu_g\beta$, 10^{-48}	β, 10^{-30} esu		
OCs	*a*	ν_{eg}, kK	*b*	*c*	*d*	*e*	μ_{eg}, D	refs	λ_L, N m	*f*	*g*	*h*	refs
1	H	31	3.14		12.2			113, 114					
	D		3.1					115	1907	5.27	*1.70*		115
2	C	26	3.6	3.5	3.5			66					
	H	36	4.2		(9 ± 2)			113, 114					
	N		4.0					115	1907	7.60	*1.90*		115
	N								1318		1.96		116
	N								1064		2.03		117
	N								1064		2.19		41
	N								1064		2.27		118
	N								1064		2.29		119
	B								1064		2.00		120
	D								1907		2.2		41
3	H	35	2.75		7.1(S_2)			113, 114					
	H	42	2.75		6.3(S_3)			113, 114					
	N		2.8					115	1907	2.24	*0.80*		115
4	B	25	6.9		13			113, 114, 121−124					
	H	36	6.45		13.5(S_1)			113, 114, 122−124					
	H				13.4(S_3)			113, 114					
	D	24.57	6.2					115	1907	74.4	*12.00*		115
5	B	29	6.3		14			121					
	B	29	5.8	5.0	14			66					
	DME	27		5.7	12			66					
	D	28	6.2	6.1	15			125	1907		(9.6 ± 0.5)		126
	D								1370		(11.8 ± 0.3)		126
	D								1064		(16.9 ± 0.4)		126
	D								910		(25 ± 1)		126
	D								830		(40 ± 3)		126
	D	28.25	7.0					127	1064	114	*16.29*		127
	D		6.2					128	1064	104.78	*16.90*		128
	D	28.33	7.13				5.08	46	1907	85.56	*12.00*		46
	D								1064	206.77	*29.00*		46
	DCM	28.57	6.2					127	1064	105	*16.93*		127
	A	27.40	6.2					115	1907	57	*9.19*		115
	A	27.17	7.3					127	1064	189	*25.89*		127
	CHL	28.82						132	1907	53	*8.28*		129
	CHL								1064			34	132
	CHL								1064		(23 ± 3)		43, 44
	CHL	28.74	6.4					127	1064	107	*16.72*		127
	EA	27.93	6.7					127	1064	152	*22.69*		127
	THF	27.62	7.1					127	1064	152	*21.41*		127
	AN	27.32	6.2					127	1064	181	*29.19*		127
	M	27.03	6.1					127	1064	195	*31.97*		127
	M		6.2					41	1064	213.9	*34.50*		41
	M								1064		36.0		119
	M								1064		34.6		54
	M								1064		(34.5 ± 4.0)		130
	DMF	26.18	7.3					127	1064	219	*30.00*		127
	DMSO		{6.00÷6.23}					131	1890	286	*{47.67÷45.91}*		131
6	B	26	6.9		15			113, 114, 121−124					
	B	26		5.1	13			66					

DOI: 10.1021/jp512342y
J. Phys. Chem. B XXXX, XXX, XXX−XXX

Table 3. continued

	solvent		μ_g, D		μ_e, D				λ_L,	$\mu_g\beta$, 10^{-48}	β, 10^{-30} esu		
OCs	*a*	ν_{eg}, kK	*b*	*c*	*d*	*e*	μ_{eg}, D	refs	N m	*f*	*g*	*h*	refs
	H	44	6.85		14.3(S_2)			113, 114, 122−124					
	H				11.8(S_3)								
	DME	26		5.0	12			66					
	DMSO		{6.73÷6.93}					131	1890	355	{51.23÷52.75}		131
	A	26.60	6.4					115	1907	76.8	12.00		115
	CHL	27.03						132	1064	143			133
	CHL								1907	94			132
	CHL								1064			72	132
	D	26.18	7.14				5.34	46	1907	157.08	22.00		46
	D								1064	406.98	57.00		46
7	DMSO		{5.92}					131	1890	79	{13.34}		131
8	D	23	6.6		12.5	(11.1÷14.9)		66, 125					
	DMSO		{6.60}					131	1890	94	{14.24}		131
	CTC								1064		6.7		134
	CHL								1064		7.6		134
	DCM								1064		8.0		134
	AN								1064		7.2		134
	M								1064		7.1		134
9	H	36	5.6		13.3(S_2)			113, 114					
	DMSO		{5.60}					131	1890	129	{23.04}		131
10	B	24	7.7		18			121					
	B	19	7.7			17.9		135					
	CHL	22.83	6.5					129	1907	325	50.00		129
	CHL								1060		(219 ± 38)		42
11	H	28	6.95		14			121					
	CHL	27.47	6.0					129	1907	138	23.00		133
	CHL	22.73						132	1907	419	69.83		132
	CHL								1064			1552	132
12	B	24	6.5		22			121					
	B	18	6.5			23.4		135					
	A								1060	(262 ± 36)			42
	CHL	24.88	5.1					115	1907	204	40.00		133
	CHL								1064		(53.7÷70.4)		136
13	B	23	7.1		26.5			121					
	B	18	7.1			25.1		135					
	A	23.15	7.10				8.41	46	1064	3195	450.0		129
	A								1064		(453 ± 91)		42, 119
	DMSO								1890		(591 ± 12)		137
	CHL	23.42	6.6					115	1907	481.8	73.00		138, 133
	CHL	22.88						132	1907	553	83.79		132
	CHL	23.26						138	1064			2209	132
14	D	25	7.1		20			121					
	D	21	7.1			(20.2÷21.2)		135					
	DMSO								1890	820	(115 ± 23)		137
	CHL	26.18	5.7					115	1907	205.2	36.00		133
15	B	28	8.0		25			66					
	CTC	22.12						139					
	DMSO	20.00						139					
	CHL								1064	1270			133
16	B	25	6.0		23			121					
	B	18	6.0			22.4		135					
	CHL	32.05	5.0					129	1907	120	24.00		129
17	B	25	6.0		24			129					
	B	18	6.0			22		135					
	CHL	25.64	5.5					129, 132	1907	304	55.27		132
	CHL								1907	275	50.00		129
	CHL								1064			554	132

DOI: 10.1021/jp512342y
J. Phys. Chem. B XXXX, XXX, XXX−XXX

Table 3. continued

	solvent		μ_g, D		μ_e, D					$\mu_g\beta$, 10^{-48}	β, 10^{-30} esu		
OCs	*a*	ν_{eg}, kK	*b*	*c*	*d*	*e*	μ_{eg}, D	refs	λ_L, N m	*f*	*g*	*h*	refs
18	B	31	6.0		16.5		121						
	B	25	6.0			(13.0÷15.3)	135						
	CHL								1340		(47 ± 3)		140, 141
	CHL								1064		(62 ± 4)		140, 141

[a]Legend of solvents: A = acetone; AN = acetonitrile; B = benzene; C = cyclohexane; CHL = chloroform; CTC = carbon tetrachloride; D = 1,4-dioxane; DCM = dichloromethane; DME = dimethoxyethane; DMF = dimethylformammide; DMSO = dimethylsuphoxide; EA = ethyl acetate; H = hexane; M = methanol; N = neat; THF = tetrahydrofuran. [b]Electric dipole moment in the ground state from dielectric measurements. Values reported in braces refer to unknown or unverified solvent. [c]Electric dipole moment in the ground state from electrochromic absorption measurements. [d]Electric dipole moment in the excited state from electrochromic absorption measurements. [e]Electric dipole moment in the excited state from electrochromic fluorescence measurements. [f]From electric field induced second harmonic (EFISH; also known as DC SHG) measurements. [g]When in italics, the value is obtained combining columns b, c, and f. [h]From Hyper−Rayleigh scattering (HRS) measurements.

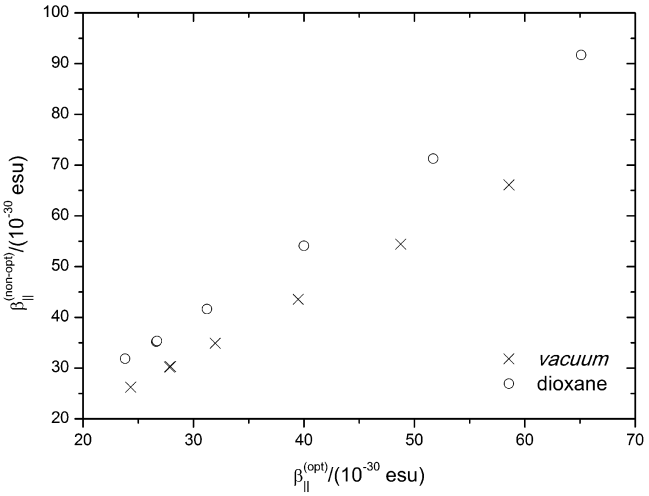

Figure 1. Comparison of the results of $\beta_{\parallel}$ computed in vacuo and in 1,4-dioxane (including local field effects). On the axis of abscissae and on the axis of ordinates, we have reported $\beta_{\parallel}$ computed with the geometry optimized at CAM-B3LYP/aug-cc-pVTZ and with the geometry optimized at B3LYP/6-31+G*, respectively.

B3LYP/6-31+G* level as a function of the respective values of $\beta_{\parallel}$ calculated optimizing the geometry at the same level of theory of the property calculation (CAM-B3LYP/aug-cc-pVDZ). In Figure 1 we plot the case of CAM-B3LYP/aug-cc-pVTZ, but analogue pictures are obtained for all the investigated functionals and basis sets. The trends can be fitted (by means of the least-squares approach) with straight lines, with good approximation ($R^2 > 0.999$). The fitting becomes practically perfect ($R^2 > 0.9999$) by using a parabolic model. This means that different geometries lead to equivalent results, at least concerning general trends and solvatochromic shifts, which are the main concern of the present study. Therefore, these results suggest that a computationally effective procedure may be based on a lower level (e.g., B3LYP/6-31+G*) geometry optimizations and, possibly, solvent effects, and subsequently the electric properties may be evaluated by CAM-B3LYP/aug-cc-pVDZ or SNSD (aug-cc-pVTZ or SNST if feasible) computations. This is actually the protocol we will further validate in the next section.

6.2. Benchmarking against Experiment. We have repeated the same calculations done for *p*-nitroaniline for the rest of the in OCs in Chart 1 and compared the values obtained

Table 4. Comparison between Different Calculated $\mu^*\cdot\tilde{\beta}_{vec}$ Products and the Experimental Data $\mu\beta_{\parallel}$ for Some Neutral (N) and Cationic (C) Organic Chromophores (see Chart 2)[a]

					$(\mu^*\cdot\tilde{\beta}_{vec})$, 10^{-48} esu				$\mu\beta_{\parallel}$, 10^{-48} esu		
OC	solvent	$f_{(LO)}$	$f_{(PCM)}$	λ_L, nm	2sm	vac	PCM	SMD	SMD[b]	exp	refs
N1-n	D	1.2028	1.0845	1907	84	129	156	272	(202)	157	46
	DMSO	1.2009	1.0688	1890	202	112	338	248	(233)	355	131
N1-c	"	"	1.0680	1890	50	48	97	97	(97)	94	131
N2-n	CHL	1.2105	1.0649	1064	926	610	1536	1343	(1181)	1524	132
N2-c	"	"	1.0571	1340	224	226	300	318	(324)	282	140, 141
	"	"	1.0571	1064	275	280	385	439	(416)	372	140, 141
N3-n	"	"	1.0663	1064	805	400	1400	812	(742)	1424	79
N3-c	"	"	1.0499	1907	177	300	420	272	(523)	419	132
N4-n	"	"	1.0616	1907	1104	1068	581	1879	(1675)	553	132
N4-c	DMSO	1.2009	1.0510	1890	591	302	855	954	(903)	820	137
C1-a	CHL	1.2105	1.0456	1907	−448	892	173	532	(575)	180	142
C1-b	"	"	1.0408	1907	−859	1894	210	1280	(1223)	213	142
C2-a	"	"	1.0483	1907	−186	398	226	313	(176)	236	142
C2-b	"	"	1.0462	1907	−393	940	237	535	(441)	243	142

[a]Legend of symbols and acronyms: $f_{(LO)}$ (local field factor referring to Lorentz−Onsager spherical model), $f_{(PCM)}$ (local field factor calculated through polarizable continuum model), λ_L (laser frequency), 2sm (two-state model), vac (calculation in vacuo), PCM (polarizable continuum model), SMD (Truhlar and coworkers' solvation model), and exp (experimental data). [b]The values in parentheses refer to SP SMD calculations done with IEF-PCM optimized geometries.

DOI: 10.1021/jp512342y
J. Phys. Chem. B XXXX, XXX, XXX−XXX

for the first-order hyperpolarizability directly with the experimental (EFISH) ones. In the literature, a lot of experimental data can be found concerning the determination of the first-order hyperpolarizability, in different solvents and with different laser sources for the selected systems. We collect these data in Table 3. We have also accounted for three different kinds of radii, viz., universal force field (UFF),[107] Pauling–Merz–Singh–Kollman's (PMSK),[108] and Bondi's (B),[109] that can be employed for building the cavity in the dielectric. From such a comparison and after a standard statistical analysis (based on the evaluation of the discrepancies and standard deviations of the computed values with respect to the experimental ones), we have defined some important guidelines for the computational evaluation of the target property.

The results confirm the findings of the previous section and earlier works.[110−112] Concerning the parallel hyperpolarizability and the product $\boldsymbol{\mu}^*\cdot\tilde{\boldsymbol{\beta}}_{vec}$, we find that the capability of predicting the experimental values of DFT is strongly affected by the choice of both the functional and the basis set. B3LYP is not suitable for the calculation of the molecular electric properties, especially for large molecules, as its average percent error with respect to the experiment is ca. ±70%. The error decreases dramatically when PBE0 functional is employed (ca. ±30%) Long-range corrected functionals perform better than their hybrid counterparts (e.g., we find CAM-B3LYP giving errors under ca. 15%). The predictability increases in the following order: B3LYP ≪ PBE0 < M06-2X ≈ ωB97X < CAM-B3LYP.

Concerning the choice of the basis set for the computation of the molecular electric properties, the employment of Pople's basis sets should be avoided, whereas the aug-cc-pVTZ and SNST basis sets give excellent results, but they can be too expensive in computational terms, especially if we want to obtain the properties starting from the geometries optimized with the same basis set. The aug-cc-pVDZ and SNSD basis sets are particularly effective for computing electrical properties, whereas the 6-31+G* basis set can be used only to optimize the geometries. Furthermore, UFF *radii* represent the best choice for building the cavities in the solvent, although the differences with respect to the results obtained employing the other *radii* are less than 10%. Therefore, according to our benchmarking, the best protocol for the computational determination of first-order hyperpolarizabilities at DFT level is B3LYP or CAM-B3LYP/6-31+G* (for the geometry optimization) and CAM-B3LYP/SNSD, using PCM with UFF *radii* for properties.

6.3. Application of the Protocol to a Set of Neutral and Cationic Systems. The findings of the previous benchmarking have been employed for calculating the $\boldsymbol{\mu}^*\cdot\tilde{\boldsymbol{\beta}}_{vec}$ product of some middle-sized OCs (Chart 2): 8 neutral OCs (a subset of the previous ones) and 4 cationic OCs, in various solvents and excited by different laser sources, covering quite a wide range of values. We also compare the results with those obtained using more simplified models often found in the literature:

- the local field factors as described both with the approximated LO model (polarizable point dipole in the center of a spherical cavity) and through the more reliable PCM(UFF) cavity,
- the $\boldsymbol{\mu}^*\cdot\tilde{\boldsymbol{\beta}}_{vec}$ products at different levels of theory, viz., employing the two-state model not accounting for solvent effects, and two computational approaches which model the cavity accounting for the molecular shape (i.e., IEF-PCM(UFF) and SMD).

All the calculations (including those for obtaining the quantities needed for the two-state model evaluation) were run within a (TD-)DFT CAM-B3LYP/SNSD framework. These data, as well as the experimental ones, are shown in Table 4. (The values of $\beta_{\parallel}$ coming from the application of the two-state model were corrected with the $f_{(PCM)}$ in order to obtain $\tilde{\beta}_{\parallel}$.) Our results suggest that

1. Solvation must be included in the predictive computational protocol, since the results obtained in vacuo are in strong disagreement with the experiments: in the case of NOCs and COCs (but for C2-a), the values are overestimated and underestimated, respectively.
2. The approximate LO approach for the estimation of local field factors leads to an overestimation of the local field factors when compared with the PCM results.
3. The two-state model fails in the prediction of the properties of COCs, whereas it seems to work better for the NOCs (with relative errors larger than 20%, in absolute value). In all cases (except N4-n) it underestimates the correct value. Such an approach also requires very delicate and tricky measurements when applied experimentally, especially in the case of cationic systems, for which the usual methods for the determination of dipole moments cannot be applied and should be abandoned.
4. We have tested the applicability of the SCM solvation model, which has been designed for an accurate prediction of the thermochemistry in the solvated phase. Its predictability of the electronic properties is not very satisfactory, giving good results for only a few NOCs, and thus it should be avoided for the study of the properties of COCs.
5. The IEF-PCM(UFF) model, enriched by the inclusion of local field effects, provided excellent predictions both for NOCs and for COCs (errors under the 5%, in absolute value).

Figure 2 shows the comparison between the results obtained applying the two-state model and the DFT/PCM approach to

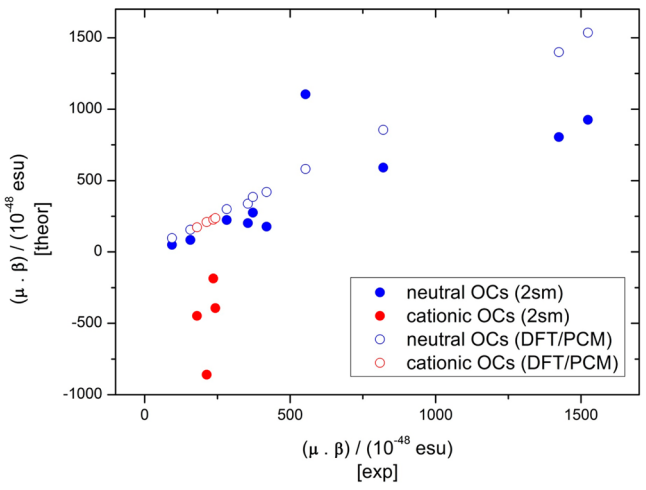

Figure 2. Comparison between the results obtained applying the two-state model (filled circles) and the DFT/PCM approach (empty circles) to the neutral (blue) and cationic (red) OCs of Chart 2, with respect to the experiments.

DOI: 10.1021/jp512342y
J. Phys. Chem. B XXXX, XXX, XXX−XXX

the NOCs and COCs of Chart 2, with respect to the experiments. The two-state model (filled circles) is capable of predicting the experimental values for NOCs in the limit of small $\mu\beta_{\parallel}$, whereas it gives results far from the reference for COCs. On the contrary, the proposed DFT/PCM procedure (unfilled circle) provides a good linear fitting with respect to the experiment, for all the OCs investigated.

7. CONCLUSIONS

The main aim of this work was to study solvent effects on the first-hyperpolarizability of OCs, with particular interest for the cationic ones, which have greater importance in the design of new NLO materials. We endeavored to bridge theory and experiment, analyzing the crucial aspects of both. We designed a computational DFT/PCM procedure, which seems to give results in good agreement with the experiments. The main conclusions that can be drawn are the following:

- when evaluating computationally the first-hyperpolarizability of OCs, direct and indirect solvent effects must be included in the treatment, since solute−solvent interactions play a central role in the determination of the property and the predictions in vacuo fail;
- inclusion of solvent effects requires some caution in order to define a predictive computational tool: according to our investigation, the best results were obtained using long-range corrected functionals (e.g., CAM-B3LYP) with Pople's basis sets (e.g., 6-31+G*) for overall computations and basis sets including diffuse polarization functions (SNSD, SNST, aug-cc-pVDZ, or aug-cc-pVTZ) for electrical properties;
- furthermore, the solvent cavity and the solute electronic density must be modeled properly (the dipole in a spherical cavity approximation used in the Lorentz−Onsager model does not account for the shape and the electronic density of the solute) and local field effects must be taken into account;
- finally, the two-state model should be abandoned in favor of a computational approach based on response theory, which implicitly includes the contributions due to all excitations and is able to provide excellent results at a low computational cost for OCs of medium−large size.

■ ASSOCIATED CONTENT

Supporting Information

Computation of the electric dipole moment, isotropic polarizability, and parallel hyperpolarizability of *p*-nitroaniline, in vacuo and in solution (1,4-dioxane), at DFT/PCM(UFF) level, employing different basis sets and different functionals is available free of charge via the Internet at http://pubs.acs.org.

■ AUTHOR INFORMATION

Corresponding Authors

*(E.B.) E-mail: enrico.benassi@sns.it. Phone: +39 050 509 682. Fax: +39 050 563 513.

*(V.B.) E-mail: vincenzo.barone@sns.it. Phone: +39 050 509 134. Fax: +39 050 563 513.

Notes

The authors declare no competing financial interest.

■ ACKNOWLEDGMENTS

E.B. thanks the Italian "Ministero per l'Università e la Ricerca Scientifica e Tecnologica" for funding [FIRB 2013, RBFR13PSB6]. The technical staff of the HPC facilities of the DreamsLab centre at the SNS is also acknowledged.

■ REFERENCES

(1) Zyss, J. *Molecular Nonlinear Optics: Materials, Physics and Devices*; Academic Press: San Diego, CA, 1994.

(2) Nalwa, H. S.; Miyata, S. *Nonlinear Optics of Organic Molecules and Polymers*; CRC Press: Boca Raton, FL, 1997.

(3) Kruhlak, R. J.; Young, J. E.; Kuzyk, M. G. Loss and Correlation Measurements in Squaraine-Doped Nonlinear Polymer Optical Fibers. *SPIE Proc.* **1997**, *3147*, 118−127.

(4) Breitung, E. M.; Shu, C.-F.; McMahon, R. J. Thiazole and Thiophene Analogues of Donor−Acceptor Stilbenes: Molecular Hyperpolarizabilities and Structure−Property Relationships. *J. Am. Chem. Soc.* **2000**, *122*, 1154−1160.

(5) Marder, S. R.; Perry, J. W.; Schaefer, P. W. Synthesis of Organic Salts with Large Second-Order Optical Nonlinearities. *Science* **1989**, *245*, 626−628.

(6) Clays, K.; Wostyn, K.; Olbrechtes, G.; Persoons, A.; Watanabe, A.; Nogi, K.; Duan, X.-M.; Okada, S.; Oikawa, H.; Nakanishi, H.; et al. Fourier Analysis of the Femtosecond Hyper−Rayleigh Scattering Signal from Ionic Fluorescent Hemicyanine Dyes. *J. Opt. Soc. Am. B* **2000**, *17*, 256−265.

(7) Clays, K.; Coe, B. J. Design Strategies versus Limiting Theory for Engineering Large Second-Order Nonlinear Optical Polarizabilities in Charged Organic Molecules. *Chem. Mater.* **2003**, *15*, 642−648.

(8) Coe, B. J.; Jones, L. A.; Harrs, J. A.; Brunschwig, B. S.; Asselberghs, I.; Clays, K.; Persoons, A. Highly Unusual Effects of π-Conjugation Extension on the Molecular Linear and Quadratic Nonlinear Optical Properties of Ruthenium(II) Ammine Complexes. *J. Am. Chem. Soc.* **2003**, *125*, 862−863.

(9) Coe, B. J.; Jones, L. A.; Harrs, J. A.; Brunschwig, B. S.; Asselberghs, I.; Clays, K.; Persoons, A.; Garin, J.; Orduna, J. Highly Unusual Effects of π-Conjugation Extension on the Molecular Linear and Quadratic Nonlinear Optical Properties of Ruthenium(II) Ammine Complexes. *J. Am. Chem. Soc.* **2004**, *126*, 3880−3891.

(10) Kay, A. J.; Woolthouse, A. D.; Gainsford, G. J.; Haskell, T. G.; Barnes, T. H.; McKinnie, I. T.; Wyss, C. P. A Simple, Novel Method for the Preparation of Polymer-Tetherable, Zwitterionic Merocyanine NLO−Chromophores. *J. Mater. Chem.* **2001**, *11*, 996−1002.

(11) Pan, F.; Shing, M.; Gramlich, V.; Bosshard, C.; Gunter, P. A Novel and Perfectly Aligned Highly Electro-Optic Organic Cocrystal of a Merocyanine Dye and 2,4-Dihydroxybenzaldehyde. *J. Am. Chem. Soc.* **1996**, *118*, 6315−6316.

(12) Duan, X.-M.; Okada, S.; Oikawa, H.; Matsuda, H.; Nakanishi, H. Second-Order Hyperpolarizabilities of Organic Ionic Species. *Mol. Cryst. Liq. Cryst.* **1995**, *267*, 89−94.

(13) Marder, S. R.; Perry, J. W. Organic, Metallo-Organic, and Polymeric Materials for Nonlinear Optical Applications. *Proc. SPIE* **1994**, *2143*.

(14) Okada, S.; Masaki, A.; Matsuda, H.; Nakanishi, H.; Oikawa, H.; Kato, M.; Otsuka, M. Synthesis and Crystal Structure of a Novel Organic Ion-Complex Crystal for Second-Order Nonlinear Optics. *Jpn. J. Appl. Phys.* **1990**, *29*, 1112−1115.

(15) Wong, M. S.; Feng, P.; Martin, B.; Rolf, S.; Christian, B.; Gunter, P.; Volker, G. Novel Electro-Optic Molecular Cocrystals with Ideal Chromophoric Orientation and Large Second-Order Optical Nonlinearities. *J. Opt. Soc. Am. B* **1998**, *15*, 426−431.

(16) Feng, P.; Wong, M. S.; Volker, G.; Christian, B.; Günter, P. A Novel and Perfectly Aligned Highly Electro-Optic Organic Cocrystal of a Merocyanine Dye and 2,4-Dihydroxybenzaldehyde. *J. Am. Chem. Soc.* **1998**, *118*, 6315−6316.

(17) Duan, X.-M.; Konami, H.; Okada, S.; Oikawa, H.; Matsuda, H.; Nakanishi, H. Second-Order Hyperpolarizabilities of Stilbazolium Cations Studied by Semiempirical Calculation. *J. Phys. Chem.* **1996**, *100*, 17780−17785.

(18) Zhu, W.; Wu, G.-S. Molecular Design for Octupolar Nonlinear Optical Systems: An ab Initio Study of First Hyperpolarizabilities of

DOI: 10.1021/jp512342y
J. Phys. Chem. B XXXX, XXX, XXX−XXX

Symmetrically Heteroaromatic-Substituted Triazines. *J. Phys. Chem. A* **2001**, *105*, 9568−9574.
(19) Kelley, A. M. Frequency-Dependent First Hyperpolarizabilities from Linear Absorption Spectra. *J. Opt. Soc. Am. B* **2002**, *19*, 1890−1900.
(20) Karamanis, P.; Maroulis, G. An ab initio Study of CX3-Substitution (X = H, F, Cl, Br, I) Effects on the Static Electric Polarisability and Hyperpolarisability of Diacetylene. *J. Phys. Org. Chem.* **2011**, *24*, 588−599.
(21) Champagne, B.; Botek, E.; Nakano, M.; Nitta, T.; Yamaguchi, K. Basis Set and Electron Correlation Effects on the Polarisability and Second Hyperpolarisability of Model Open-Shell π-Conjugated Systems. *J. Chem. Phys.* **2005**, *122*, 114315.
(22) Alparone, A.; Reis, H.; Papadopoulos, M. G. Theoretical Investigation of the (Hyper)polarisabilities of Pyrrole Homologues C_4H_4XH (X = N, P, As, Sb, Bi). A Coupled-Cluster and Density Functional Theory Study. *J. Phys. Chem. A* **2006**, *110*, 5909−5918.
(23) Naves, E. S.; Castro, M. A.; Fonseca, T. L. Dynamic (hyper)polarisabilities of the Sulphur Dioxide Molecule: Coupled Cluster Calculations Including Vibrational Corrections. *J. Chem. Phys.* **2012**, *136*, 014303.
(24) Coe, J. P.; Paterson, M. J. Approaching Exact Hyper-polarisabilities via Sum-Over-States Monte Carlo Configuration Interaction. *J. Chem. Phys.* **2014**, *141*, 124118.
(25) Albert, I. D. L.; Marks, T. J.; Ratner, M. A. Rational Design of Molecules with Large Hyperpolarizabilities. Electric Field, Solvent Polarity, and Bond Length Alternation Effects on Merocyanine Dye Linear and Nonlinear Optical Properties. *J. Phys. Chem.* **1996**, *100*, 9714−9725.
(26) Capobianco, A.; Centore, R.; Noce, C.; Peluso, A. Molecular Hyperpolarizabilities of Push−Pull Chromophores: A Comparison Between Theoretical and Experimental Results. *Chem. Phys.* **2013**, *411*, 11−16.
(27) Ferrighi, L.; Frediani, L.; Cappelli, C.; Sałek, P.; Ågren, H.; Helgaker, T.; Ruud, K. Density-Functional-Theory Study of the Electric-Field-Induced Second Harmonic Generation (EFISHG) of Push−Pull Phenylpolyenes in Solution. *Chem. Phys. Lett.* **2006**, *425*, 267−272.
(28) Kobayashi, R.; Koch, H.; Jørgensen, P. Calculation of Frequency-Dependent Polarizabilities Using Coupled-Cluster Response Theory. *Chem. Phys. Lett.* **1994**, *219*, 30−35.
(29) Isborn, C. M.; Leclercq, A.; Vila, F. D.; Dalton, L. R.; Bredas, J. L.; Eichinger, B. E.; Robinson, B. H. Comparison of Static First Hyperpolarizabilities Calculated with Various Quantum Mechanical Methods. *J. Phys. Chem. A* **2007**, *111*, 1319−1327.
(30) Johnson, L. E.; Dalton, R.; Robinson, B. H. Optimizing Calculations of Electronic Excitations and Relative Hyperpolarizabilities of Electrooptic Chromophores. *Acc. Chem. Res.* **2014**, *47*, 3258−3265.
(31) Tomasi, J.; Mennucci, B.; Cammi, R. Quantum Mechanical Continuum Solvation Models. *Chem. Rev.* **2005**, *105*, 2999−3093.
(32) Mennucci, B. Polarizable Continuum Model. *WIREs Comput. Mol. Sci.* **2012**, *2*, 386.
(33) Cammi, R.; Cossi, M.; Mennucci, B.; Tomasi, J. Analytical Hartree−Fock Calculation of the Dynamical Polarizabilities α, β, and γ of Molecules in Solution. *J. Chem. Phys.* **1996**, *105*, 10556−10564.
(34) Kanis, D.; Ratner, M.; Marks, T. Design and Construction of Molecular Assemblies with Large Second−Order Optical Nonlinearities. Quantum Chemical Aspects. *Chem. Rev.* **1994**, *94*, 195−242.
(35) Kleinman, D. A. Nonlinear Dielectric Polarization in Optical Media. *Phys. Rev.* **1962**, *126*, 1977−1979.
(36) Hashimoto, H.; Nakashima, T.; Hattori, K.; Yamada, T.; Mizoguchi, T.; Koyama, Y.; Kobayashi, T. Structures and Non-Linear Optical Properties of Polar Carotenoid Analogues. *Pure Appl. Chem.* **1999**, *71*, 2225−2236.
(37) The units for the first hyperpolarizabilities may be somewhat complicated. Most authors quote β in either atomic units or electrostatic units (CGS). The dimensional analysis indicates that β possesses the units of (electric dipole moment)^3/(energy)^2:

$$1\ \text{atomic unit} = 8.206 \times 10^{-53}\ \text{C}^3\ \text{m}^3/\text{J}^2 = 8.6393 \times 10^{-33}\ \text{cm}^5/\text{esu}$$

For additional comments, see ref 34.In the following table, we have collected the equivalences between the most common unit systems where 1 statvolt = erg$^{1/2}$ cm$^{-1/2}$.

		au	SI	SI alternative	esu
E	electric field	$1\ e^{-1}\ a_0^{-1}\ E_h$	$5.142\,208 \times 10^{11}$ V m^{-1}	$5.142\,2 \times 10^{11}$ V m^{-1}	$1.715\,3 \times 10^{3}$ statvolt cm^{-1}
μ	electric dipole moment	$1\ e\ a_0$	$8.478\,358 \times 10^{-30}$ C m	$8.478\,4 \times 10^{-30}$ C m	$2.541\,8 \times 10^{-18}$ statvolt cm^2
α	electric polarisability	$1\ e^2\ a_0^2\ E_h^{-1}$	$1.648\,788 \times 10^{-41}$ C^2 m^2 J^{-1}	$1.862\,1 \times 10^{-30}$ m^3	$1.481\,7 \times 10^{-25}$ cm^3
β	electric 1st hyper–polarisability	$1\ e^3\ a_0^3\ E_h^{-2}$	$3.206\,361 \times 10^{-53}$ C^3 m^3 J^{-2}	$3.621\,3 \times 10^{-42}$ m^4 V^{-1}	$8.639\,2 \times 10^{-33}$ cm^4 statvolt^{-1}
γ	electric 2nd hyper–polarisability	$1\ e^4\ a_0^4\ E_h^{-3}$	$6.235\,377 \times 10^{-65}$ C^4 m^4 J^{-3}	$7.042\,3 \times 10^{-54}$ m^5 V^{-2}	$5.036\,7 \times 10^{-40}$ cm^5 statvolt^{-2}

Finally, we remind that

$$[\text{electric dipole moment}] = 1\ \text{debye} = 10^{-18}\ \text{esu} = 3.336 \times 10^{-30}\ \text{Cm},\ [\text{energy}] = 1\ \text{eV} = 1.602 \times 10^{-19}\ \text{J}$$

(38) Olsen, J.; Jørgensen, P. Linear and Nonlinear Response Functions for an Exact State and for an MCSCF State. *J. Chem. Phys.* **1985**, *82*, 3235−3264.
(39) Helgaker, T.; Coriani, S.; Jørgensen, P.; Kristensen, K.; Olsen, J.; Ruud, K. Recent Advances in Wave Function-Based Methods of Molecular-Property Calculations. *Chem. Rev.* **2012**, *112*, 543−631.
(40) Orr, B. J.; Ward, J. F. Perturbation Theory of the Non-Linear Optical Polarization of an Isolated System. *Mol. Phys.* **1971**, *20*, 513−526.
(41) Oudar, J. L.; Chemla, D. S. Hyperpolarizabilities of the Nitroanilines and Their Relations to the Excited State Dipole Moment. *J. Chem. Phys.* **1977**, *66*, 2664−2668.
(42) Oudar, J. L. Optical Nonlinearities of Cconjugated Molecules. Stilbene Derivatives and Highly Polar Aromatic Compounds. *J. Chem. Phys.* **1977**, *67*, 446−457.
(43) Clays, K.; Persoons, A. Hyper−Rayleigh Scattering in Solution. *Phys. Rev. Lett.* **1991**, *66*, 2980−2983.
(44) Clays, K.; Persoons, A. Hyper−Rayleigh Scattering in Solution. *Rev. Sci. Instrum.* **1992**, *63*, 3285−3289.
(45) Li, D. Q.; Ratner, M. A.; Marks, T. J. Molecular and Macromolecular Nonlinear Optical Materials. Probing Architecture/Electronic Structure/Frequency Doubling Relationships via an SCF-LCAO MECI π Electron Formalism. *J. Am. Chem. Soc.* **1988**, *110*, 1707−1715.
(46) Paley, M. S.; Harris, J. M.; Looser, H.; Baumert, J. C.; Bjorklund, G. C.; Jundt, D.; Twieg, R. J. A Solvatochromic Method for Determining Second-Order Polarizabilities of Organic Molecules. *J. Org. Chem.* **1989**, *54*, 3774−3778.
(47) Bosshard, Ch.; Knöpfle, G.; Prêtre, P.; Günter, P. Second-Order Polarizabilities of Nitropyridine Derivatives Determined with Electric-Field-Induced Second-Harmonic Generation and a Solvatochromic Method: A Comparative Study. *J. Appl. Phys.* **1992**, *71*, 1594−1605.
(48) Willetts, A.; Rice, J. E.; Burland, D. M.; Shelton, D. P. Problems in the Comparison of Theoretical and Experimental Hyperpolarizabilities. *J. Chem. Phys.* **1992**, *97*, 7590−7599.
(49) Bruni, S.; Cariati, E.; Cariati, F.; Porta, F. A.; Quinci, S.; Roberto, D. Determination of the Quadratic Hyperpolarizability of Trans-4-[4-(Dimethylamino)Styryl]Pyridine and 5-Dimethylamino-1,10-Phenanthroline from Solvatochromism of Absorption and Fluorescence Spectra: a Comparison with the Electric-Field-Induced Second-Harmonic Generation Technique. *Spectrochim. Acta A* **2001**, *57*, 1417−1426.
(50) Carlotti, B.; Flamini, R.; Kikaš, I.; Mazzucato, U.; Spalletti, A. Intramolecular Charge Transfer, Solvatochromism and Hyperpolarizability

DOI: 10.1021/jp512342y
J. Phys. Chem. B XXXX, XXX, XXX−XXX

of Compounds Bearing Ethenylene or Ethynylene Bridges. *Chem. Phys.* **2012**, *407*, 9−19.
(51) Meyers, F.; Marder, S. R.; Pierce, B. M.; Brédas, J.-L. Electric Field Modulated Nonlinear Optical Properties of Donor−Acceptor Polyenes: Sum-Over-States Investigation of the Relationship between Molecular Polarizabilities (α, β, and γ) and Bond Length Alternation. *J. Am. Chem. Soc.* **1994**, *116*, 10703−10714.
(52) Corozzi, A.; Mennucci, B.; Cammi, R.; Tomasi, J. Structure versus Solvent Effects on Nonlinear Optical Properties of Push−Pull Systems: A Quantum-Mechanical Study Based on a Polarisable Continuum Model. *J. Phys. Chem. A* **2009**, *113*, 14774−14784.
(53) Bale, D. H.; Eichinger, B. E.; Liang, W.; Li, X.; Dalton, L. R.; Robinson, B. H.; Reid, P. J. Dielectric Dependence of the First Molecular Hyperpolarizability for Electro-Optic Chromophores. *J. Phys. Chem. B* **2011**, *115*, 3505−3513.
(54) Zyss, J.; Ledoux, I. Nonlinear Optics in Multipolar Media: Theory and Experiments. *Chem. Rev.* **1994**, *94*, 77−105.
(55) Sutherland, R. L. *Handbook of Nonlinear Optics*, 2nd ed.; Marcel Dekker, Inc.: 2003.
(56) Hedestrand, G. Die Berechnung der Molekularpolarisation gelöster Stoffe bei unendlicher Verdünnung (The calculation of the molecular polarization of solute at infinite dilution). *Z. Phys. Chem.* **1929**, *B2*, 428−444 (in German).
(57) Guggenheim, E. A. The Computation of Electric Dipole Moments. *Trans. Faraday Soc.* **1951**, *47*, 573−576.
(58) Smith, W. *Electric Dipole Moments*; Butterworths Scientific Publications: London, 1965.
(59) Wilson, J. M.; Newcombe, R. J.; Denaro, A. R.; W. Rickett, R. M. *Experiments in Physical Chemistry*, 2nd ed.; Pergamon Press: Oxford, 1968.
(60) White, J. M. *Physical Chemistry Laboratory Experiments*; Prentice-Hall: Englewood Cliffs, NJ, 1975.
(61) Sine, R. J. *Physical Chemistry*; Holt-Rinehart-Winston: Orlando, 1991.
(62) Schoemaker, D. P.; Garland, C. W.; Nibler, J. W. *Experiments in Physical Chemistry*, 8th ed.; McGraw Hill: New York, 2009.
(63) Bakshiev, N. G.; Knyazhanskii, M. I.; Osipov, O. A.; Minkin, V. I.; Saidov, G. V. Experimental Determination of the Dipole Moments of Organic Molecules in Excited Electronic States. *Usp. Khim.* **1969**, *38*, 1644−1673; (in Russian) *Russ. Chem. Rev.* **1969**, *38*, 740 (English translation).
(64) Mataga, N.; Kubota, K. T. *Molecular Interactions and Electronic Spectra*; Dekker: New York, 1970.
(65) Amos, A. T.; Burrows, B. L. Solvent-Shift Effects on Electronic Spectra and Excited-State Dipole Moments and Polarizabilities. *Adv. Quantum Chem.* **1973**, *7*, 303−332.
(66) Liptay, W. Dipole Moments and Polarisabilities of Molecules In Excited Electronic States. In *Excited States*; Lim, E., Ed.; Academic Press: New York, 1973; Vol. *I*, p 129.
(67) Nicol, M. Solvent Effects on Electronic Spectra. *Appl. Spectrosc. Rev.* **1974**, *8*, 183−227.
(68) Mataga, N.; Kaifu, Y.; Koizumi, M. Solvent Effetcts upon Fluorescence Spectra and the Dipole Moments of Excited Molecules. *Bull. Chem. Soc. Jpn.* **1956**, *29*, 465−470 and references therein.
(69) Von Lippert, E. Spektroskopische Bestimmung des Dipolmomentes Aromatischer Verbindungen im Ersten Angeregten Singulettzustand (Spectroscopic Determination of the Dipole Moment of Aromatic Compounds in the First Excited Singlet State). *Ber. Bunsenges. Phys. Chem.* **1957**, *61*, 962−975 (in German); and references therein.
(70) Von Lippert, E.; Lüder, W.; Moll, F.; Nagele, E.; Boos, H.; Prigge, H.; Seibold-Blankenstein, I. Umwandlung von Elektronenanregungsenergie (Conversion of Electron Excitation Energy). *Angew. Chem.* **1961**, *73*, 695−706 (in German).
(71) McRae, E. G. Solvent Effects on Merocyanine Spectra. *Spectrochim. Acta, Part A* **1958**, *12*, 192−210 and references therein.
(72) Bakhshiev, N. G. *Spectroscopy of Intermolecular Interactions*; Nauka: Leningrad, 1972 (in Russian) p 165; and references therein.
(73) Bilot, L.; Kawski, A. Zur Theorie des Einflusses von Lösungsmitteln auf die Elektronenspektren der Moleküle (On the Theory of the Influence of Solvents on the Electronic Spectra of Molecules). *Z. Naturforsch. A* **1962**, *17a*, 621−627 (in German).
(74) Kawski, A.; Gryczynski, I.; Jung, C.; Reckner, K. R. Experimentelle und Quantenchemische Untersuchungen der Dipolmomente von Substituierten Stilbenen im Ersten Angeregten Singulettzustand (Experimental and Quantum Chemical Studies of the Dipole Moments of Substituted Stilbenes in the First Excited Singlet State). *Z. Naturforsch. A* **1977**, *32a*, 420−425 (in German).
(75) Ravi, M.; Samanta, A.; Radhakrishnan, T. P. Excited State Dipole Moments from an Efficient Analysis of Solvatochromic Stokes Shift Data. *J. Phys. Chem.* **1994**, *98*, 9133−9136.
(76) From a linear regression of the solvatochromic shift as a function of an opportune polarity function, we can obtain a relation involving the dipole moments and the radius of Onsager's spherical cavity.
(77) Chamma, A.; Viallet, P. Détermination du Moment Dipolaire d'une Molécule Dans un État Excité Singulet: Application à l'Indole, au Benzimidazole et à l'Indazole (Determination of the Dipole Moment of a Molecule in a Singlet Excited State: Application to Indole, to Benzimidazole and to Indazole). *C. R. Acad. Sci. C* **1970**, *270*, 1901−1904 (in French).
(78) Abribat, G.; Viallet, P. Détermination du Moment Dipolaire d'une Molécule Dans un État Excité Singulet: Application à Quelques Méthyl Indole (Determination of the Dipole Moment of a Molecule in a Singlet Excited State: Application to Some Methylindole). *C. R. Acad. Sci. C* **1970**, *271*, 1029−1032.
(79) Onsager, L. Electric Moments of Molecules in Liquids. *J. Am. Chem. Soc.* **1936**, *58*, 1486−1493.
(80) Cammi, R.; Cappelli, C.; Corni, S.; Tomasi, J. On the Calculation of Infrared Intensities in Solution within the Polarizable Continuum Model. *J. Phys. Chem. A* **2000**, *104*, 9874−9879.
(81) Cammi, R.; Mennucci, B.; Tomasi, J. An Attempt To Bridge the Gap between Computation and Experiment for Nonlinear Optical Properties: Macroscopic Susceptibilities in Solution. *J. Phys. Chem. A* **2000**, *104*, 4690−4698.
(82) Cammi, R.; Mennucci, B.; Tomasi, J. On the Calculation of Local Field Factors for Microscopic Static Hyperpolarizabilities of Molecules in Solution with the Aid of Quantum-Mechanical Methods. *J. Phys. Chem. A* **1998**, *102*, 870−875.
(83) Mennucci, B.; Cammi, R.; Tomasi, J. Excited States and Solvatochromic Shifts Within a Nonequilibrium Solvation Approach: A New Formulation of the Integral Equation Formalism Method at the Self-Consistent Field, Configuration Interaction, and Multiconfiguration Self-Consistent Field Level. *J. Chem. Phys.* **1998**, *109*, 2798−2807.
(84) Mikkelsen, K. V.; Luo, Y.; Ågren, H.; Jørgensen, P. Solvent Induced Polarisabilities and Hyperpolarisabilities of Para-Nitroaniline Studied by Reaction Field Linear Response Theory. *J. Chem. Phys.* **1994**, *100*, 8240−8250.
(85) Egidi, F.; Giovannini, T.; Piccardo, M.; Bloino, J.; Cappelli, C.; Barone, V. Stereoelectronic, Vibrational, and Environmental Contributions to Polarizabilities of Large Molecular Systems: A Feasible Anharmonic Protocol. *J. Chem. Theory Comput.* **2014**, *10*, 2456−2464.
(86) Pipolo, S.; Corni, S.; Cammi, R. The Cavity Electromagnetic Field Within the Polarisable Continuum Model of Solvation. *J. Chem. Phys.* **2014**, *140*, 164114.
(87) Sylvester-Hvid, K. O.; Mikkelsen, K. V.; Jonsson, D.; Norman, P.; Ågren, H. Nonlinear Optical Response of Molecules in a Nonequilibrium Solvation Model. *J. Chem. Phys.* **1998**, *109*, 5576−5584.
(88) Sekino, H.; Bartlett, R. J. Frequency Dependent Nonlinear Optical Properties of Molecules. *J. Chem. Phys.* **1986**, *85*, 976−989.
(89) Rice, J. E.; Amos, R. D.; Colwell, S. M.; Handy, N. C.; Sanz, J. Frequency Dependent Hyperpolarizabilities with Application to Formaldehyde and Methyl Fluoride. *J. Chem. Phys.* **1990**, *93*, 8828−8839.
(90) Marenich, A. V.; Cramer, C. J.; Truhlar, D. G. Universal Solvation Model Based on Solute Electron Density and on a

DOI: 10.1021/jp512342y
J. Phys. Chem. B XXXX, XXX, XXX−XXX

Continuum Model of the Solvent Defined by the Bulk Dielectric Constant and Atomic Surface Tensions. *J. Phys. Chem. B* **2009**, *113*, 6378−6396.
(91) Frisch, M. J.; Trucks, G. W.; Schlegel, H. B.; Scuseria, G. E.; Robb, M. A.; Cheeseman, J. R.; Scalmani, G.; Barone, V.; Mennucci, B.; Petersson, G. A.; Nakatsuji, H.; Caricato, M.; Li, X.; Hratchian, H. P.; Izmaylov, A. F.; Bloino, J.; Zheng, G.; Sonnenberg, J. L.; Hada, M.; Ehara, M.; Toyota, K.; Fukuda, R.; Hasegawa, J.; Ishida, M.; Nakajima, T.; Honda, Y.; Kitao, O.; Nakai, H.; Vreven, T.; Montgomery, J. A., Jr.; Peralta, J. E.; Ogliaro, F.; Bearpark, M.; Heyd, J. J.; Brothers, E.; Kudin, K. N.; Staroverov, V. N.; Kobayashi, R.; Normand, J.; Raghavachari, K.; Rendell, A.; Burant, J. C.; Iyengar, S. S.; Tomasi, J.; Cossi, M.; Rega, N.; Millam, J. M.; Klene, M.; Knox, J. E.; Cross, J. B.; Bakken, V.; Adamo, C.; Jaramillo, J.; Gomperts, R.; Stratmann, R. E.; Yazyev, O.; Austin, A. J.; Cammi, R.; Pomelli, C.; Ochterski, J. W.; Martin, R. L.; Morokuma, K.; Zakrzewski, V. G.; Voth, G. A.; Salvador, P.; Dannenberg, J. J.; Dapprich, S.; Daniels, A. D.; Farkas, O.; Foresman, J. B.; Ortiz, J. V.; Cioslowski, J.; Fox, D. J. *Gaussian 09*, revision D.01; Gaussian, Inc.: Wallingford, CT, 2009.
(92) Becke, A. D. Density-Functional Thermochemistry. III. The Role of Exact Exchange. *J. Chem. Phys.* **1993**, *98*, 5648−5652.
(93) Adamo, C.; Barone, V. Toward Reliable Density Functional Methods Without Adjustable Parameters: The PBE0Model. *J. Chem. Phys.* **1999**, *110*, 6158−6170.
(94) Zhao, Y.; Truhlar, D. G. The M06 Suite of Density Functionals for Main Group Thermochemistry, Thermochemical Kinetics, Noncovalent Interactions, Excited States, and Transition Elements: Two New Functionals and Systematic Testing of Four M06-Class Functionals and 12 Other Functionals. *Theor. Chem. Acc.* **2008**, *120*, 215−241.
(95) Yanai, T.; Tew, D.; Handy, N. A New Hybrid Exchange-Correlation Functional Using the Coulomb-Attenuating Method (CAM-B3LYP). *Chem. Phys. Lett.* **2004**, *393*, 51−57.
(96) Chai, J.-D.; Head-Gordon, M. Systematic Optimization of Long-Range Corrected Hybrid Density Functionals. *J. Chem. Phys.* **2008**, *128*, 084106.
(97) Dunning, T. H., Jr. Gaussian Basis Sets for Use in Correlated Molecular Calculations. I. The Atoms Boron Through Neon and Hydrogen. *J. Chem. Phys.* **1989**, *90*, 1007−1023.
(98) Kendall, R. A.; Dunning, T. H., Jr.; Harrison, R. J. Electron Affinities of the First-Row Atoms Revisited. Systematic Basis Sets and Wave Functions. *J. Chem. Phys.* **1992**, *96*, 6796−6806.
(99) Woon, D. E.; Dunning, T. H., Jr. Gaussian-Basis Sets for Use in Correlated Molecular Calculations. 3. The Atoms Aluminum Through Argon. *J. Chem. Phys.* **1993**, *98*, 1358−1371.
(100) Peterson, K. A.; Woon, D. E.; Dunning, T. H., Jr. Benchmark Calculations with Correlated Molecular Wave Functions. IV. The Classical Barrier Height of the H+H2 → H2+H Reaction. *J. Chem. Phys.* **1994**, *100*, 7410−7415.
(101) Wilson, A. K.; van Mourik, T.; Dunning, T. H., Jr. Gaussian Basis Sets for Use in Correlated Molecular Calculations. VI. Sextuple Zeta Correlation Consistent Basis Sets for Boron Through Neon. *J. Mol. Struct. (Theochem)* **1996**, *388*, 339−349.
(102) Kendall, R. A.; Dunning, T. H., Jr.; Harrison, R. J. Electron Affinities of the First-Row Atoms Revisited. Systematic Basis Sets and Wave Functions. *J. Chem. Phys.* **1992**, *96*, 6796−6806.
(103) Woon, D. E.; Dunning, T. H., Jr. Gaussian-Basis Sets for Use in Correlated Molecular Calculations. 3. The Atoms Aluminum Through Argon. *J. Chem. Phys.* **1993**, *98*, 1358−1371.
(104) http://compchem.sns.it/downloads.
(105) Tomasi, J.; Mennucci, B.; Cancès, E. The IEF Version of the PCM Solvation Method: an Overview of a New Method Addressed to Study Molecular Solutes at the QM ab initio Level. *J. Mol. Struct.: Theochem.* **1999**, *464*, 211−226.
(106) Scalmani, G.; Frisch, M. J. Continuous Surface Charge Polarizable Continuum Models of Solvation. I. General Formalism. *J. Chem. Phys.* **2010**, *132*, 114110.
(107) Rappé, A. K.; Casewit, C. J.; Colwell, K. S.; Goddard, W. A.; Skiff, W. M. UFF, a Full Periodic Table Force Field for Molecular Mechanics and Molecular Dynamics Simulations. *J. Am. Chem. Soc.* **1992**, *114*, 10024−10035.
(108) Singh, U. C.; Kollman, P. A. An Approach to Computing Electrostatic Charges for Molecules. *J. Comput. Chem.* **1984**, *5*, 129−145.
(109) Bondi, A. van der Waals Volumes and Radii. *J. Phys. Chem.* **1964**, *68*, 441−451.
(110) Limacher, P. A.; Mikkelsen, K. V.; Luthi, H. P. On the Accurate Calculation of Polarisabilities and Second Hyperpolarisabilities of Polyacetylene Oligomer Chains Using the CAM-B3LYP Density Functional. *J. Chem. Phys.* **2009**, *130*, 194114.
(111) Bulik, I. W.; Zalesny, R.; Bartkowiak, W.; Luis, J. M.; Kirtman, B.; Scuseria, G. E.; Avramopoulos, A.; Reis, H.; Papadopoulos, M. G. Performance of Density Functional Theory in Computing Nonresonant Vibrational (Hyper)Polarisabilities. *J. Comput. Chem.* **2013**, *34*, 1775−1784.
(112) Baranowska-Laczkowska, A.; Bartkowiak, W.; Gora, R. W.; Pawlowski, F.; Zalesny, R. On the Performance of Long-Range-Corrected Density Functional Theory and Reduced-size Polarized LPol-n Basis Sets in Computations of Electric Dipole (Hyper)-Polarisabilities of π-Conjugated Molecules. *J. Comput. Chem.* **2013**, *34*, 819−826.
(113) Lenhart, H.; Wagnière, G. Experimentelle und Theoretische Untersuchung der Angeregten Elektronenzustände Einiger Substituierter Benzole (Experimental and Theoretical Investigation of the Excited Electronic States of Some Substituted Benzenes). *Helv. Chim. Acta* **1963**, *46*, 1314−1316 (in German).
(114) Lenhart, H.; Wagnière, G. Experimentelle und Theoretische Untersuchung der Angeregten Elektronenzustände Einiger Substituierter Benzole: Berichtigung zur gleichnamigen (Experimental and Theoretical Investigation of the Excited Electronic States of Some Substituted Benzenes: Adjustment on the Same). *Helv. Chim. Acta* **1968**, *51*, 204−212 (in German).
(115) Cheng, L.-T.; Tam, W.; Stevenson, S. H.; Meredith, G. R.; Rikken, G.; Marder, S. R. Experimental Investigations of Organic Molecular Nonlinear Optical Polarizabilities. 1. Methods and Results on Benzene and Stilbene Derivatives. *J. Phys. Chem.* **1991**, *95*, 10631−10643.
(116) Levine, B. F. Donor−Acceptor Charge Transfer Contributions to the Second Order Hyperpolarizability. *Chem. Phys. Lett.* **1976**, *37*, 516−520.
(117) Levine, B. F.; Bethea, C. G. Second and Third Order Hyperpolarizabilities of Organic Molecules. *J. Chem. Phys.* **1975**, *63*, 2666−2682.
(118) Oudar, J. L.; Chemla, D. S.; Batifol, E. Optical Nonlinearities of Various Substituted Benzene Molecules in the Liquid State, and Comparison with Solid State Nonlinear Susceptibilities. *J. Chem. Phys.* **1977**, *67*, 1626−1635.
(119) Oudar, J. L.; Le Person, H. Second-Order Polarizabilities of Some Aromatic Molecules. *Opt. Commun.* **1975**, *15*, 258−262; Errata. *Opt. Commun.* **1976**, *18*, 410−411.
(120) Levine, B. F.; Bethea, C. G. Molecular Hyperpolarizabilities Determined From Conjugated and Nonconjugated Organic Liquids. *Appl. Phys. Lett.* **1974**, *24*, 445−447.
(121) Czekalla, J.; Wick, G. Die Bestimmung von Absoluten Übergangsmomentrichtungen und von Dipolmomenten angeregter Moleküle aus Messungen des Elektrischen Dichroismus. II. Ergebnisse (The Determination of Absolute Transition Moment Directions of Dipole Moments of Excited Molecules from Measurements of the Electric Dichroism. II. Results). *Z. Elektrochemie* **1961**, *65*, 727−734 (in German).
(122) Lenhart, H. Vortrag Symposium über Farbenchemie, Basel, Juli 1960 (Lecture Symposium on Colour Chemistry, Basel, July 1960). *Chimia* **1961**, *15*, 20 (in German).
(123) Lenhart, H. Beeinflussung der Lichtabsorption Organischer Farbstoffe Durch Äussere Elektrische Felder I. Theoretische Betrachtung (Influence of Light Absorption of Organic Dyes by External Electric Fields I. Theoretical Considerations. *Helv. Chim. Acta* **1961**, *44*, 447−457 (in German).

DOI: 10.1021/jp512342y
J. Phys. Chem. B XXXX, XXX, XXX−XXX

(124) Lenhart, H. Beeinflussung der Lichtabsorption Organischer Farbstoffe Durch Äussere Elektrische Felder II. Experimentelle Untersuchungen an Polyenen (Influence of Light Absorption of Organic Dyes by External Electric Fields II. Experimental Studies of Polyenes). *Helv. Chim. Acta* **1961**, *44*, 457−467 (in German).
(125) Liptay, W.; Eberlein, W.; Weisenberger, H.; Elflein, O. Die Beeinflussung der Optischen Absorption von Molekülen Durch ein Äußeres Elektrisches Feld. V. Übergangsmomentrichtungen und Dipolmomente der Niedrigen Elektronenzustände in 4-Nitranilin, 1-Nitro-3,5-diaminobenzol, 3,5-Dinitroanilin, Carbazol und 3,6-Dinitrocarbazol (The Influence of the Optical Absorption of Molecules Across an External Electric Field. V. Transition Moment Directions and Dipole Moments of the Low Electron States in 4-Nitroaniline, 1-Nitro-3,5-Diaminobenzene, 3,5-Dinitroaniline, Carbazole and 3,6-Dinitrocarbazole). *Ber. Bunsen-Ges.* **1967**, *71*, 548−560 (in German).
(126) Teng, C. C.; Garito, A. F. Dispersion of the Nonlinear Second-Order Optical Susceptibility of Organic Systems. *Phys. Rev. B* **1983**, *28*, 6766−6773.
(127) Stähelin, M.; Burland, D. M.; Rice, J. E. Solvent Dependence of the Second Order Hyperpolarizability in p-Nitroaniline. *Chem. Phys. Lett.* **1992**, *191*, 245−250.
(128) Sinha, H. K.; Yates, K. Effects of Positions of Donor and Acceptor Type Substituents on Ground- and Excited-State Charge Transfer: Electrochromism of Some Benzene Derivatives. *J. Am. Chem. Soc.* **1991**, *113*, 6062−6067.
(129) Cheng, L.-T.; Tam, W.; Marder, S. R.; Stiegman, A. E.; Rikken, G.; Spangler, C. W. Experimental Investigations of Organic Molecular Nonlinear Optical Polarizabilities. 2. A Study of Conjugation Dependences. *J. Phys. Chem.* **1991**, *95*, 10643−10652.
(130) Böttcher, C. J. F. *Theory of Electrodynamics*; Elsevier: Amsterdam, 1973.
(131) Dulcic, A.; Sauteret, C. The Regularities Observed in the Second Order Hyperpolarizabilities of Variously Disubstituted Benzenes. *J. Chem. Phys.* **1978**, *69*, 3453−3457 and references therein.
(132) Flipse, M. C.; de Jonge, R.; Woudenberg, R. H.; Marsman, A. W.; van Walree, C. A.; Jenneskens, L. W. The Determination of First Hyperpolarizabilities β Using Hyper-Rayleigh Scattering: a Caveat. *Chem. Phys. Lett.* **1995**, *245*, 297−303.
(133) Ulman, A.; Willand, C. S.; Köhler, W.; Robello, D. R.; Williams, D. J.; Handley, L. New Sulfonyl-Containing Materials for Nonlinear Optics: Semiempirical Calculations, Synthesis, and Properties. *J. Am. Chem. Soc.* **1990**, *112*, 7083−7090.
(134) Robinson, D. W.; Long, C. A. Quadratic hyperpolarizability of 4-(Dimethylamino)Benzonitrile in Solvents of Differing Polarity. *J. Phys. Chem.* **1993**, *97*, 7540−7542.
(135) Czekalla, J.; Liptay, W.; Meyer, K. O. Die Beeinflussung der Fluoreszenz von Molekülen Durch ein Äußeres Elektrisches Feld II. Bestimmung von Dipolmomenten Angeregter Moleküle (The Effect on the Fluorescence of Molecules by an External Electric Field II. Determination of Dipole Moments of Excited Molecules). *Ber. Bunsen-Ges.* **1963**, *67*, 465−470 (in German).
(136) Li, D. Q.; Marks, T. J.; Ratner, M. A. Nonlinear Optical Phenomena in Conjugated Organic Chromophores: Theoretical Investigations Via a π-Electron Formalism. *J. Phys. Chem.* **1992**, *96*, 4325−4336 and references therein.
(137) Dulcic, A.; Flytzanis, C.; Tang, C. L.; Pépin, D.; Fétizon, M.; Hoppiliard, Y. Length Dependence of the Second-Order Optical Nonlinearity in Conjugated Hydrocarbons. *J. Chem. Phys.* **1981**, *74*, 1559−1563.
(138) Marder, S. R.; Beratan, D. N.; Cheng, L.-T. Approaches for Optimizing the First Electronic Hyperpolarizability of Conjugated Organic Molecules. *Science* **1991**, *252*, 103−106.
(139) Hoffman, D. P.; Mathies, R. A. Photoexcited Structural Dynamics of an Azobenzene Analog 4-Nitro-4′-Dimethylamino-Azobenzene From Femtosecond Stimulated Raman. *Phys. Chem. Chem. Phys.* **2012**, *14*, 6298−6306.
(140) Ledoux, I.; Zyss, J.; Jutand, A.; Amatore, C. Nonlinear Optical Properties of Asymmetric Polyphenyls: Efficiency Versus Transparency Trade-Off. *Chem. Phys.* **1991**, *150*, 117−123.
(141) Zyss, J.; Ledoux, I.; Bertauld, M.; Toupet, E. Dimethylamino-cyanobiphenyl (DMACB): A New Optimized Molecular Crystal for Quadratic Nonlinear Optics in the Visible. *Chem. Phys.* **1991**, *150*, 125−135.
(142) Fortuna, C. G.; Bonaccorso, C.; Qamar, F.; Anu, A.; Ledoux, I.; Musumarra, G. Synthesis and NLO Properties of New Trans 2-(Thiophen-2-yl)Vinyl Heteroaromatic Iodides. *Org. Biomol. Chem.* **2011**, *9*, 1608−1613.

DOI: 10.1021/jp512342y
J. Phys. Chem. B XXXX, XXX, XXX−XXX